IHCs	CDX2 (%)	CGA (%)	SYN (%)
Appendix	98.7	4.5	14.3
Stomach	77.1	30.0	17.2

Conclusions: The diffuse nuclear staining pattern of SATB2 is consistently identified in appendiceal GCCs and absent in gastric SRCCs that are metastatic to the ovary. Compared to traditional markers, SATB2 is a novel useful marker in identifying primary anatomic sites in metastatic signet ring cell lesions in the ovary.

1280 Assessment of Clinical and Pathological Factors Contributing to Negative LEEP

Youran Zou, Gloria Zhang, Charles V Biscotti, Jerome L Belinson, Bin Yang. Cleveland Clinic, Cleveland, OH.

Background: Accurate diagnosis of squamous dysplasia on cervical biopsy is important not only for guiding treatment of HSIL lesions but also for preventing over treatment. We have reviewed a large cohort of LEEP cases and assessed clinical and pathological factors contributing to negative LEEP.

Design: All LEEP cases from 2007, 2009, 2013, and 2015 were identified in our pathology archive. Prior diagnosis, p16 immunostaining results, and LEEP diagnosis were recorded. Factors affecting clinical decisions including cervical cytology results, HPV testing and others were noted. LACK of HSIL (either benign or CIN1) defined as negative LEEP. Cases with glandular abnormalities have been excluded from this study. Consistent application of p16 immunostain by most of our pathologists began in 2012. To determine whether p16 immunostain affects negative LEEP rate, we compared negative LEEP rate in 2007-2009 (prior to p16 application) and in 2013-2015 (post p16 application).

Results: A total of 1,256 LEEP cases were identified, consisting of 674 cases prior to p16 and 582 cases post p16 application. Negative LEEP rate was 42.7% (288/674) prior to p16 and was 36.1% (210/582) post p16 application (p=0.02). Among negative LEEP cases, pathologists' contribution (CIN2+ diagnosis on biopsy with subsequent negative LEEP) was 61.1% (176/288) prior to p16 and 54.8% (115/210) post p16 application. Clinicians' contribution (performed LEEP either with no biopsy or biopsy diagnosis as benign or CIN1) was 39.9% (112/288) prior to p16 and 46.2% (95/210) post p16 application.

Conclusions: Negative LEEP is contributed both by pathologists and by clinicians. Application of p16 has decreased the negative LEEP rate contributed by pathologists, presumably with more accurate CIN2+ diagnosis. Conversely clinicians' contribution to negative LEEP has relatively increased after wide application of p16 for HSIL lesions.

1281 Invasive Implants of Ovarian Serous Borderline Tumor: Significant Association with *KRAS* but Not *BRAF* Mutation

Tao Zuo, Serena Wong, Natalia Buza, Pei Hui. Yale University, New Haven, CT.

Background: In contrast to non-invasive implants, invasive implants of serous borderline tumor/atypical proliferative serous tumor (SBT/APST) are associated with adverse clinical outcome and currently classified as low-grade serous carcinoma by the 2014 WHO classification. Somatic mutations in *KRAS* and *BRAF* have been reported in more than 50% of SBT/APST. In this study, we investigated *KRAS* and *BRAF* mutation frequencies in the two types of SBT/APST implants in correlation with clinical outcome.

Design: Thirty-seven implants of SBT/APST from 34 patients were included. The implants were reviewed and reclassified according to the 2014 WHO criteria into 18 invasive and 19 non-invasive implants. DNA was extracted from microdissected tissue samples and subjected to PCR amplification followed by single-strand conformation polymorphism analysis (SSCP) to detect the presence of *KRAS* exon 2 and *BRAF* V600E mutations. The implant type and presence of KRAS/BRAF mutations were correlated with clinical follow-up data.

Results: *KRAS* and *BRAF* mutation analyses were informative in all but one non-invasive implant (Table 1). *KRAS* mutation was found in 11 of 18 invasive implants (61%) and 4 of 18 non-invasive implants (22%) (p=0.018; *Chi Square*). *BRAF V600E* mutation was seen in 1 of 19 non-invasive implants (5%) and none of 18 invasive implants harbored *BRAF V600E* mutation (0%). Two patients had two implants (each one invasive and one non-invasive) analyzed and *KRAS* mutation was seen only in the invasive implants but not in the non-invasive implants in both patients. Invasive implants were more frequently associated with high stage disease (p=0.007; *Chi Square*). Eleven of 19 patients (58%) with stage IIIC disease were found to have *KRAS* mutation, while only one patient with stage IIB had the mutation. However, Kaplan-Meyer survival analyses did not show significant survival differences between invasive and non-invasive implants and between implants with and without *KRAS* mutation, although a prognostic trend was suggested.

	Invasive Implant (N=18)	Non-invasive Implant (N=19)	Total (N=37)
KRAS Mutation	11/18(61%)	4/18 (22%)	15/36 (42%)
BRAF Mutation	0/18 (0%)	1/19 (5%)	1/37 (3%)

Conclusions: Invasive implants of SBT/APST are significantly associated with *KRAS* mutations and a wild-type *BRAF*. PCR-SSCP is a highly sensitive and specific method for detection of *KRAS/BRAF* mutations in small tissue samples such as microscopic implants of SBT/APST. Additional studies are necessary to ascertain the prognostic values of *KRAS/BRAF* mutation analysis of implants of SBT/APST.

Head and Neck Pathology

1282 SMARCB1 (INI-1)-Deficient Sinonasal Carcinoma: A Series of 33 Cases Expanding the Morphological and Clinicopathological Spectrum of a Recently Described Entity

Abbas Agaimy, Arndt Hartmann, Cristina R Antonescu, Simon Chiosea, Samir K El-Mofty, James Lewis, Stacey E Mills, Ann Sandison, Roderick HW Simpson, William H Westra, Justin A Bishop. University Hospital of Erlangen, Erlangen, Germany; Memorial Sloan Kettering Cancer Center, New York, NY; University of Pittsburgh Medical Center, Pittsburgh, PA.

Background: SMARCB1-deficient sinonasal carcinoma is a recently described sinonasal tumor entity characterized by loss of nuclear SMARCB1 (INI1).

Design: To more fully characterize the clinicopathological spectrum of this proposed entity, we analyzed 33 cases collected from multiple medical centers.

Results: Both sexes were affected equally (age range: 19 to 87 yrs; median, 52). All patients presented with locally advanced disease (T4, n=27) involving the sinuses and variably the nasal cavity. Twenty-five patients received surgery and/or radiochemotherapy with curative intent. At last follow-up, 58% of patients died of disease (0 to 102 months; median, 16), 2 were alive with disease, and 1 died of unrelated cause. Only 6 patients (29%) were alive without disease (11-115 months; median, 34). Original diagnoses of archival cases were most often sinonasal undifferentiated carcinoma (n=12) and non-keratinizing/basaloid squamous cell carcinoma (n=4). Histologically, most tumors displayed either predominantly basaloid (55%) or plasmacytoid/rhabdoid (38%) morphology. The plasmacytoid/rhabdoid form consisted of sheets of tumor cells with eccentric nuclei and eosinophilic cytoplasm, while similar cells were rare and singly distributed in the basaloid variant. Glandular differentiation was seen in a few tumors. Squamous differentiation and surface dysplasia were absent. By immunohistochemistry (IHC), the tumors were positive for pankeratin (97%), CK5 (65%), p63 (50%) and CK7 (43%). NUT IHC was negative. Epstein-Barr virus and high risk human papillomavirus were not detected by in situ hybridization. Loss of SMARCB1 (INI1) expression was confirmed for all 33 tumors by IHC. SMARCB1 deletions were detected in 19/23 cases by FISH.

Conclusions: SMARCB1-deficient sinonasal carcinoma represents a distinctive emerging poorly/undifferentiated sinonasal carcinoma that 1) cannot be better classified as another specific tumor type, 2) has consistent (albeit variable) histopathological findings, and 3) demonstrates an aggressive clinical course. This diagnosis should be considered in any difficult-to-classify sinonasal carcinoma, in order to optimize therapy and to further delineate this probably underdiagnosed disease.

1283 Extranodal Lymphoid Neoplasms of the Head and Neck: A Retrospective Analysis

Yahya Al-Ghamdi, Faizan Malik, Smita Patel, Brett Mahon, Paolo Gattuso. Rush University Medical Center, Chicago, IL.

Background: Lymphoid neoplasms of head and neck (HN) account for 12-15% of all head and neck tumors and 5% of all malignancies. This study aimed to investigate the clinicopathological features of lymphoid neoplasms arising in mucosal sites of HN. Additionally, considering its therapeutic target and its association with a more favorable outcome in diffuse large B-cell lymphomas (DLBCL), CD30 immunoexpression was assessed.

Design: We searched the archives of our department from 2000 to 2016 for lymphoid neoplasms diagnosed at HN sites. The cases were divided to two groups: Primary - localized without bone marrow involvement; Secondary - diagnosed in the HN with bone marrow involvement or relapsed cases of a known lymphoma. Clinical characteristics, autoimmune association, histologic subtype, and CD30 immunoexpression were analyzed.

Results: Sixty cases were retrieved, including 31 women and 29 men. The mean age was 59.78 years (range: 16–91). Among 49 cases whose medical charts were available, 35 were primary and 14 were secondary. The sites of involvement include tonsils (n=25; 41.6%), nasopharynx (n=12; 20%), base of the tongue (n=10, 16.7%), larynx (n=7; 11.7%), maxillary sinuses (n=3; 5%), and oral mucosa (n=3; 5%). Histologic subtypes include DLBCL (n=22; 36.7%), mantle cell lymphoma (n=8; 13.3%), marginal zone lymphoma (n=7;11.7%), peripheral T-cell lymphoma (n=6; 10%), follicular lymphoma (n=4; 6.7%), extranodal NK/T cell lymphoma (n=4; 6.7%), small lymphocytic lymphoma/chronic lymphocytic leukemia (n=3, 5%), unclassifiable B-cell lymphoma, intermediate between DLBCL and Burkitt lymphoma (n=2; 3.3%). In addition, there were single cases of plasmablastic lymphoma, Burkitt lymphoma, and ALK-negative anaplastic large cell lymphoma. Among 16 DLBCL cases assessed for CD30 immunoexpression, 3 were positive. Two DLBCL cases were EBV positive by in-situ hybridization. Eleven patients had an autoimmune association, including hypothyroidism (n=4), rheumatoid arthritis (n=3), inflammatory bowel disease (n=2), Sjögren's syndrome (n=1), and autoimmune hepatitis (n=1). Five of these 11 patients had a primary lymphoma. An unclassified T-cell lymphoma developed in a patient with combined variant immunodeficiency. Two cases were associated with human immunodeficiency virus infection.

Conclusions: Both B- and T-cell lymphoid neoplasms of head and neck are not uncommon and should always be considered in the differential diagnosis. Most cases in our study were primary lymphomas. The most common site of involvement was the Waldeyer ring. Our findings suggest an immune dysregulation association.

1284 The Value of *PRKD1* E710D Sequencing of May-Grünwald-Giemsa Stained Cytology Specimens in Separating Polymorphous Low-Grade Adenocarcinoma from Adenoid Cystic Carcinoma and Pleomorphic Adenoma

Simon Andreasen, Morten Grauslund, Linea C Melchior, Irene Wessel, Katalin Kiss, Tina K Agander. Copenhagen University Hospital Rigshospitalet, Copenhagen, Denmark; Zealand University Hospital, Køge, Denmark.

Background: Polymorphous low-grade adenocarcinoma (PLGA), termed polymorphous adenocarcinoma in the upcoming WHO classification, is a salivary gland tumor most frequently arising in the palate. On cytological specimens, it has a significant overlap with adenoid cystic carcinoma (ACC) and pleomorphic adenoma (PA), but the prognosis and clinical management is markedly different. The recent discovery of the *PRKD1* E710D point mutation in PLGA could help in making an accurate preoperative diagnosis on fine needle aspiration (FNA) material. We investigate the value of the *PRKD1* E710D point mutation in May-Grünwald-Giemsa (MGG)-stained smears and their corresponding surgical specimens in a series of PLGA, ACC, and PA.

Design: Archival FNAs from 16 PLGAs, 18 ACCs, and 24 PAs originating from the palate were retrieved along with corresponding surgical specimens. DNA was extracted from FNA material and surgical specimens. Dideoxynucleotide sequencing of *PRKD1* exon 15, encoding E710D, was performed in nested PCR reactions and assessed blinded to diagnosis.

Results: Eight FNAs from PLGA contained E710D point mutations, c.2130 A>T (Fig. 1A) and c.2130 A>C (Fig. 1B) in 3 and 5 cases, respectively. The remaining 7 cases showed no E710D mutations.

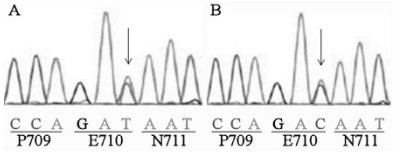

All FNAs from ACCs and PAs had normal E710D. Sequencing of the corresponding surgical specimens showed identical E710D mutations as the FNA in all cases of all three tumor categories. The specificity of *PRKD1* E710D point mutation in separating PLGA from ACC and PA was 100% (95%CI:91.6-100%), the sensitivity in diagnosing PLGA was 53.3% (26.6-78.7%), the positive predictive value 100% (63-100%), and the negative predictive value 85.7% (72.7-94%).

Conclusions: *PRKD1* E710D sequencing in MGG stained FNA is feasible and highly specific in separating PLGA from ACC and PA, whereas the sensitivity is only moderate. This can be useful in the diagnostic work-up and planning of surgery.

1285 Clinical and Biological Significance of Common Mutational Genotypes of Thyroid Follicular Neoplasia

Joseph F Annunziata, Anna Banizs, Christina M Narick, Sara Jackson, Jan F Silverman, Sydney Finkelstein. Allegheny General Hospital, Pittsburgh, PA; Interpace Diagnostics, Pittsburgh, PA.

Background: Somatically acquired oncogene mutational change is a fundamental to thyroid neoplasia. While certain mutations confer highly predictable degrees of biological aggressiveness, other mutation types are less predictable. We report on our large experience thyroid nodule mutational change correlated with cytology and RNA expression level determination to better understand neoplastic progression according to specific mutation type.

Design: 5,210 indeterminate thyroid nodule needle aspirates underwent mutational analysis for common mutations (BRAF, HRAS, KRAS, NRAS, PIK3CA, PAX8/PPAR and RET/PTC translocation) by next generation sequencing (Illumina). Cytology diagnosis was based on pathology report diagnoses (Bethesda diagnostic categories). As an independent predictor of neoplastic behavior, a panel of 10 microRNAs was developed. Mutation type was correlated with cytology diagnosis and microRNA prediction of clinical aggressiveness.

Results: Oncogenic mutations were detected in 1100/5,210 (21.1%) of the cases. The majority were point mutations (95.3%) and the remainder were translocations (4.7%). Virtually all nodules displayed a single genotype for this mutation panel. RAS genes accounted for most point mutations (n=736) distributed as NRAS (57.0%), HRAS (26.7%) and KRAS (16.3%). Mutations were seen in across cytology categories, the relative distribution varied according to specific genotype. B-V was dominated by BRAF V600E (40.9%) but included all genotypes. B-III and B-IV manifested all genotypes with relatively greater content of ras gene mutations (16.7% and 15.6 %) and all BRAF point mutations outside of V600E. MicroRNA (miR) expression classifier yielded a four level quantitative measure of increasing malignancy risk (very low 99+% NPV, low 94% NPV, moderate 74% PPV, high 99+% PPV). Individual mutational genotypes within specific oncogenes displayed unique malignancy risk profiles correlating with cytology.

Conclusions: Cytology prediction of malignancy risk is challenging in the earlier stages of neoplastic progression. RAS gene mutations, the most common oncogene alteration, are diverse and not equivalent. While certain mutations are highly predictive of cancer, the majority of individual mutation genotypes show biological heterogeneity. Combining RNA expression profiling with mutation determination leads to more information to base risk assessment.

1286 Plasmacytoid Cells (PLC) in Pleomorphic Salivary Adenomas (PA) and Plasmacytoid Myoepitheliomas (PM) Are Probably Not of Myoepithelial Cell (MC) Origin and May Reflect Cells Capable of Undergoing Epithelial/Mesenchymal Transition (EMT)

Prokopios Argyris, Mark Lingen, Elizabeth A Bilodeau, Ioannis Koutlas. Oral and Maxillofacial Pathology, University of Minnesota, Minneapolis, MN; University of Chicago, Chicago, IL; University of Pittsburgh, School of Dental Medicine, Pittsburgh, PA.

Background: Most salivary gland tumor classifications regard PLC in PA and PM as modified neoplastic MC. However, this origin is not definitive as PLC fail to demonstrate myogenic properties when evaluated histochemically, immunohistochemically and ultrastructurally. Positivity for CK7, p63 and S100 has been cited to support MC origin. However, these markers are not specific or pathognomonic for MC. In addition, immunoreactivity for calponin has been reportedly weak and there is consistent a-SMA negativity. We have observed strong WT-1 and D2-40 PLC reactivity, primarily at the periphery of the tumor nests and in close proximity to stromal areas rich in glycosaminoglycans suggesting the possibility of EMT.

Design: We investigated the immunoprofile of PLC for the expression of CK14, p40, h-caldesmon, DOG1 as well as EMT-associated proteins SOX10, SNAIL/SLUG and e-cadherin in FFPE specimens of PLC-predominant PA and PM. Normal minor salivary glands were used as internal controls.

Results: Rare focal positivity for CK14 was observed while p40 expression was generally negative except in one case that showed sporadic nuclear immunoreactivity. H-caldesmon and DOG1 expression were consistently and uniformly negative. PLC demonstrated a diffuse nuclear SOX10 immunopositivity. Variable nuclear and cytoplasmic SNAIL/SLUG immunoreactivity was observed while there was weak or absent e-cadherin expression.

Conclusions: PLC failed to demonstrate uniform expression patterns of traditional and novel MC IHC markers. Additionally, the observed pattern of expression of some of these markers, in conjunction with the pattern of staining observed for SNAIL/SLUG, SOX10 and e-cadherin, suggest that PLC may be capable of undergoing EMT. Therefore, the use of the term PM may need to be reconsidered. Furthermore, in the absence of DOG1 immunoreactivity, an intercalated duct origin for PLC is not favored. Lastly, PM should be categorized either as a subtype of PA or in the group of monomorphic adenomas.

1287 Gene Expression Profiling by NanoString Discriminates Papillary Carcinoma, Follicular Carcinoma and Normal Thyroid Tissue

Hanan Armanious, Iyare Izevbaye, Benjamin Adam. University of Alberta, Edmonton, AB, Canada.

Background: Evaluation of thyroid nodules with fine needle aspiration biopsy (FNAB) is the most widely used technique to identify malignancy. However, up to 15% of FNAB will have a diagnosis of atypia of unknown significance (AUS). Several studies have proposed molecular testing as an adjunct strategy for increasing diagnostic accuracy. However, previous efforts have lacked the required sensitivity and negative predictive value (NPV) to prevent surgical intervention.

Design: Using NanoString nCounter, we analyzed the expression of 83 genes previously described as exhibiting aberrant expression in thyroid malignancies. We characterized 28 FFPE tumor samples, including 12 classical papillary carcinomas (PTC) and 14 follicular carcinomas (FTC), and 6 normal thyroid samples. Hierarchical clustering by Euclidean distance was used to identify targets that could potentially discriminate between different tumor types. Fold change was used to identify genes with significant differential expression and receiver operating characteristic (ROC) curve analysis was used to assess the diagnostic performance of this refined gene subset.

Results: Heat map analysis demonstrated loose clustering of normal thyroid, PTC and FTC samples with inclusion of the entire 83-gene panel.

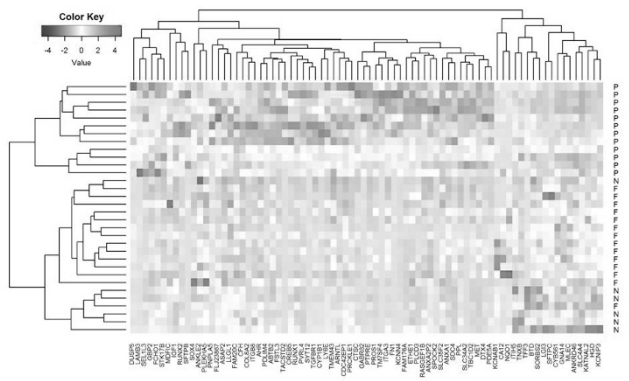

Selecting targets with the greatest fold change differences between tissue types resulted in a refined 13-gene subset. This subset demonstrated perfect diagnostic classification of PTC vs. FTC and PTC vs. normal (AUC, sensitivity, specificity, PPV, NPV and accuracy all 100%) and good classification of FTC vs. normal (AUC 81%, sensitivity 83%, specificity 79%, PPV 63%, NPV 92%, accuracy 80%).

Conclusions: These results demonstrate promising utility in distinguishing PTC, FTC and normal thyroid samples using FFPE-based gene expression technology. Following validation, this assay may be used to help discriminate FNAB cases of AUS and thus guide clinical management.

1288 Non-Invasive Follicular Thyroid Neoplasm with Papillary-Like Nuclear Features (NIFTP): A Single Institutional Review with Emphasis on Tumor Prevalence

Nabil Ashraf, Rongqin Ren, Cora Uram-Tuculescu, Celeste N Powers, Adele O Kraft. Virginia Commonwealth University Health System, Richmond, VA.

Background: Noninvasive encapsulated follicular variant of papillary thyroid carcinoma (NIFTP) is a recently proposed designation for a subset of follicular variant of papillary thyroid carcinoma (FVPTC) cases defined by strict histopathological criteria and with an indolent biologic behavior when compared to invasive FVPTC. Given the currently limited published data and in an effort to assess NIFTP prevalence and tumor characteristics a retrospective review of FVPTC cases was performed at our institution.
Design: A computerized search of all cases of papillary thyroid carcinomas (PTC) from 2006 to 2016 was performed at our institution. FVPTC cases with reported capsular and/or angiolymphatic invasion, metastatic and/or recurrent tumors were excluded. Slides from the remaining FVPTC cases were examined by four pathologists to assess the published NIFTP major and minor inclusion and exclusion criteria for possible re-classification. Tumor characteristics including size, focality, encapsulation, and background thyroid abnormalities as well as additional clinical parameters and outcomes were noted.
Results: A total of 218 thyroidectomy specimens with primary, nonmetastatic PTC, were identified. Of these 73 were diagnosed as FVPTC and 42 were excluded due to reported capsular and/or angiolymphatic invasion. After review 17 cases of the remaining 31, met the published criteria for NIFTP. All the15 NIFTP patients with available follow up information were disease-free (range: 2 months to 9 years, mean 2.7 years).

Cases	Number (%)
Total # of PTC	218
Total # of FVPTC	73 (33%)
FVPTC without capsular and angioinvasion	31 (14%)
Total # NIFTP	17 (8%)

Reasons for exclusion*	Number of cases
Infiltrative borders	10
True papillae > 1%	10
Lack of encapsulation or demarcation	5
Psammomma bodies	4
Tumor Necrosis	0
High mitotic activity	0
Nuclear score < 2	0
Features of other PTC variants	0

*Some potential NIFTP cases failed multiple criteria
Conclusions: At our institution 8% of primary, nonmetastatic PTC cases identified on thyroidectomies met the proposed published criteria for the NIFTP category.

1289 Pleomorphic Adenoma: Benign, Recurrent and Malignant Transformation

Munita Bal, Swati Thorat, Swapnil Rane, Asawari Patil, Shubhada Kane, Rajiv Kumar, Gouri Pantavaidya, Jai Prakash Agarwal, Anil DCruz. Tata Memorial Centre, Mumbai, Maharashtra, India.

Background: Pleomorphic adenoma (PA) is an enigmatic tumor with unique pathological features and an unpredictable tendency towards malignant transformation in a subset of cases. Our aim was to study the clinicopathologic spectrum of benign, recurrent and malignant PA diagnosed at our centre.
Design: A retrospective review of clinical and pathologic findings of head and neck PA cases diagnosed from 2004-2013 was undertaken.
Results: 187 PA cases were studied and subdivided into 3 groups (G): G1, non-recurrent PA (n=94); G2, recurrent PA (n=23); and G3, PA with malignant transformation (PAMT) (n=70). Median time-to-recurrence and time-to-malignant transformation was 6.5 years and 19 years in G2 and G3 cohorts, respectively. G2 cases had an earlier median age of onset, male predominance, larger mean tumor size, stroma-rich histology and greater cellular atypia, mitotic rate, satellite nodules and extra-parenchymal spread (EPS) than G1 cases. Among G3, 46 cases were de novo (PAMT at first presentation) while 24 were secondary (following a previously documented/resected PA); commonest histology was salivary duct carcinoma and myoepithelial carcinoma in de novo and secondary groups, respectively. Larger size, higher T stage, increased margin positivity and shorter disease free survival was seen in secondary versus de novo tumors.

PLEOMORPHIC ADENOMA WITH MALIGNANT TRANSFORMATION-HISTOLOGIC TYPES	N=70
A. CARCINOMA EX-PLEOMORPHIC ADENOMA	66 (94.2%)
a. SALIVARY DUCT CARCINOMA, NOT OTHERWISE SPECIFIED	29
b. SALIVARY DUCT CARCINOMA, SARCOMATOID VARIANT	4
c. ADENOCARCINOMA, NOT OTHERWISE SPECIFIED	16
d. MYOEPITHELIAL CARCINOMA	15
e. MUCOEPIDERMOID CARCINOMA	1
f. SQUAMOUS CELL CARCINOMA	1
B. CARCINOSARCOMA EX-PLEOMORPHIC ADENOMA	2 (2.9%)
C. SARCOMA EX-PLEOMORPHIC ADENOMA	2 (2.9%)
a. CHONDROSARCOMA	1
b. PLEOMORPHIC SARCOMA	1

High T stage, EPS, high grade, margin positivity and nodal metastasis was seen in 91%, 89%, 80%, 28% and 39% G3 cases, respectively. Intracapsular carcinoma and minimally-invasive PAMT (i.e. extracapsular invasion ≤ 1.5 mm) were associated with favorable prognosis when compared to widely-invasive PAMT (p value=0.02).
Conclusions: PA is a unique clinicopathologic entity. Recurrent PA exhibit atypical pathological features. PAMT display a wide pathologic spectrum, aggressive clinicopathologic features and a poor prognosis. Intracapsular and minimally-invasive PAMTs are a favorable prognostic category among the malignant PA cohort.

1290 PARP1 Overexpression in Merkel Cell Carcinoma and Its Potential Clinical Implications

Diana Bell, Shirley Y Su, Bonnie Glisson, Merril Kies, Victor G Prieto, Renata Ferrarotto. MD Anderson Cancer Center, Houston, TX.

Background: Merkel cell carcinoma (MCC) is an aggressive high-grade neuroendocrine skin tumor frequently associated with the Merkel cell Polyomavirus (MCPyV). The genetic landscape of MCPyV negative tumors mirrors small cell lung cancer (SmCC), majority harboring mutations in *TP53* and *RB1* and scarce actionable mutations in oncogenes. Patients with recurrent/ metastatic disease are treated with similar SmCC chemotherapy schemas. Based on profiling data of SmCC revealing a high expression of DNA repair proteins, particularly PARP1, and promising anti-tumor activity of PARP inhibitors in SmCC patients in early clinical trials, we aimed to evaluate the expression of PARP1 in MCC.
Design: A cohort of 19 patients diagnosed with MCC and with tissue available for histological studies was identified. IHC analysis for PARP1 was performed in 4 micron paraffin embedded tissue sections; only tumor tissue with strong nuclear staining in > 10% of the neoplastic cells were considered positive. Polyoma virus status was evaluated by staining with anti- MCPyV antibody in the tissue specimens. Patient's characteristics were collected retrospectively.
Results: The median age at diagnosis was 71 years old, 74% (14/19) of patients were male, 74% (14/19) had a primary tumor in the head and neck region. PARP1 and MCPyV expression 42% tumors (8/19) were MCPyU positive. Strong PARP1 IHC staining was observed in the majority of cases (15/19 or 79%).

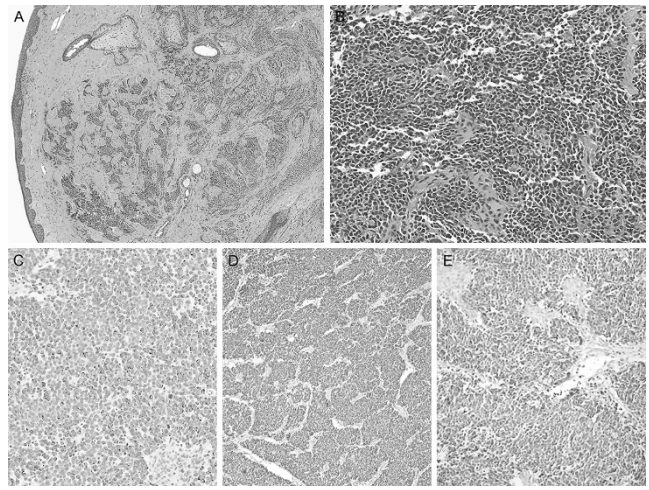

A, B- H&E of Merkel cell carcinoma of eyelid. C- Phenotypically the tumor display characteristical perinuclear pattern when stained with anti-CK20 antibody. Diffuse strong nuclear positivity with anti- PARP1 (D) and MCPyV (E) antibodies). There was no statistical correlation between PARP1 overexpression and MCPyU status or primary site of disease.
Conclusions: As observed in small cell lung cancer, PARP1 overexpression is prevalent in MCC suggesting underlying defects in DNA-repair in this tumor type. MCC represents a major unmet need that poses the additional challenging of affecting preferentially immunosuppressed individuals, limiting the use of the emerging immunotherapy option. Given the early signs of activity of PARP inhibitors in SCLC, we believe this class of agents deserves further investigation in MCC patients.

1291 Hyalinizing Clear Cell Carcinoma of the Oropharynx and Other Head and Neck Sites Is a p16-Positive Tumor: A Potential Pitfall

Justin A Bishop, William H Westra. The Johns Hopkins University, Baltimore, MD.

Background: Hyalinizing clear cell carcinoma (HCCC) is a low-grade malignancy that most commonly arises in minor salivary glands of the oropharynx. *EWSR1-ATF1* gene fusions appear to be specific for this neoplasm, and testing for *EWSR1-ATF1* has expanded the histologic spectrum of HCCC. As one important example, many HCCCs have a predominant squamous phenotype with relatively few clear cells - a finding that can cause considerable confusion with squamous cell carcinoma. P16 immunohistochemistry to determine HPV status has become standard practice for all oropharyngeal carcinomas showing squamous differentiation. The purpose of this study was to determine whether HCCCs are p16-positive and thus contribute to further diagnostic error.
Design: The surgical pathology archives of The Johns Hopkins Hospital were searched for cases of HCCC. All cases were evaluated with p16 and p40 immunohistochemistry, high risk HPV RNA in situ hybridization (ISH), and *EWSR1* gene break-apart fluorescence ISH.

Results: Nine HCCCs were identified. All harbored a *EWSR1* rearrangement. Six patients were women and 3 were men. They ranged in age from 40 to 80 years (mean, 57). The HCCCs arose in the tongue base (n=5), nasopharynx (n=2), oral tongue (n=1) and retromolar trigone (n=1). All cases were diffusely p40-positive. Each case demonstrated clear cells, but the proportion was highly variable (20 to 80%, mean 52%), with 6 of 9 cases having ≤50% clear cells. Two were originally diagnosed as squamous cell carcinoma (SCC), and 2 as mucoepidermoid carcinoma. One patient originally diagnosed as SCC was planning to undergo chemoradiation before the diagnosis was correctly overturned, and the other patient diagnosed as SCC had already undergone chemoradiation with no response. All 9 cases were p16 positive. Staining was predominantly nuclear. P16 staining was present in ≥70% of cells in 2 cases, 50-70% of cells in 2 cases, and 10–49% of cells in 5 cases. All cases were negative for high-risk HPV.

Conclusions: HCCCs often show well-developed squamous features, often lack prominent clear cell features, frequently arise in the oropharynx, and are invariably p16 positive. This profile may cause confusion with squamous cell carcinoma in general, and with HPV-related oropharyngeal carcinoma specifically, with significant clinical consequences. P16 staining is not to be taken as unequivocal evidence of an HPV-related squamous cell carcinoma, even for carcinomas showing squamous differentiation and originating in the oropharynx.

1292 Sinonasal HPV-Related Carcinoma with Adenoid Cystic Carcinoma-Like Features: An Expanded Series of 34 Cases

Justin A Bishop, Simon Andreasen, Martin Bullock, Douglas Gnepp, Carmen Gomez, Alessandro Franchi, Katalin Kiss, James Lewis, Kelly Magliocca, Ann Sandison, William H Westra. Johns Hopkins, Baltimore, MD; Copenhagen University, Copenhagen, Denmark; Dalhousie University, Halifax, Canada; University Pathologists, Fall River, MA; University of Miami, Miami, FL; University of Florence, Florence, Italy; Vanderbilt, Nashville, TN; Emory, Atlanta, GA; Charing Cross Hospital, London, United Kingdom.

Background: We recently described HPV-related carcinoma with adenoid cystic-like features (HPV-ACC), a peculiar neoplasm restricted to the sinonasal tract with features of a surface-derived and salivary gland carcinoma. Given the limited number of cases in the original series, the full clinicopathologic spectrum of this neoplasm was unclear. Here, we present an updated multiinstitutional series.

Design: All HPV-ACCs were pulled from the authors' files. IHC for p16 and myoepithelial markers S100, actin, calponin, p63, and/or p40 was performed along with RNA ISH for HPV (type 33 and a high-risk cocktail). Follow-up was obtained via electronic medial records.

Results: 34 cases of HPV-ACC were collected, all from the sinonasal tract: 22 women and 12 men from 28-90 y (mean, 53). Of 25 patients with staging information, 46% presented at stage T3 or 4. Histologically, most were predominantly solid nests of basaloid cells with numerous mitoses, necrosis, and myoepithelial features (cell clearing, spindling, matrix). Most cases also demonstrated foci of cribriform or tubular growth, with an inconspicuous population of ducts. 62% had squamous dysplasia of the surface epithelium. Novel histologic features included squamous differentiation in the invasive tumor (n=5), sarcomatoid features (n=4) including chondroid differentiation, epithelial-myoepithelial carcinoma-like patterns (n=2), and pure cribriform growth (n=2). All showed myoepitheilal differentiation by IHC and were diffusely p16+. HPV ISH was uniformly positive including 20 (59%) positive for type 33. In 28 cases with follow-up, 39% recurred locally and 7% metastasized distantly. There were no regional lymph node metastases, and no tumor-related deaths in the follow up period.

Conclusions: HPV-ACC is a distinct sinonasal neoplasm characterized by myoepithelial differentiation, frequent surface dysplasia, an association with HPV type 33, and a broader histologic spectrum than previously recognized. Although HPV-ACC often presents at high-stage and has a high-grade histologic appearance, it paradoxically behaves in a relatively indolent manner, underscoring the importance of distinguishing HPV-ACC from true adenoid cystic carcinoma and other basaloid sinonasal carcinomas.

1293 EBV-Related Nasopharyngeal Carcinoma in Native Americans of New Mexico

Cory Broehm, Angela Meisner, Marc Barry, Charles Wiggins, Therese Bocklage. University of New Mexico School of Medicine, Albuquerque, NM; University of New Mexico Health Sciences Center, Albuquerque, NM.

Background: EBV-related nasopharyngeal carcinoma (NPC) has a significantly increased prevalence among certain East Asian populations and among Alaska Natives. The prevalence among Native Americans of New Mexico, which includes a significant proportion of Navajo and Apache who are genetically and linguistically related to Athabaskan Alaska Natives, has not been systematically studied.

Design: The Surveillance, Epidemiology, and End Results (SEER) 13 Registry was queried for all cases of NPC with EBV-related histology from 1992 to 2013 in New Mexico, Seattle-Puget Sound (with a significant Native component) and the Alaska Native Tumor Registry. The age-adjusted rate of NPC/100k population for Native Americans, Hispanics, and Whites, and 95% confidence interval (CI) were calculated. Our institutional archives were queried from 2000-2016 for cases of NPC with EBV-positivity confirmed by immunohistochemistry or in-situ hybridization. Sex, age at presentation, and self-identified ancestry were recorded for each case.

Results: The SEER registry recorded 154 cases of NPC in New Mexico, including 26 in Native Americans (rate 0.840, CI 0.540-1.243), 56 in Hispanics (rate 0.392, CI 0.294-0.511), and 72 in Whites (rate 0.299, CI 0.232-0.380). 282 cases of NPC were recorded in Seattle-Puget Sound, including 16 in Native Americans (rate 1.288, CI 0.712-2.164), 10 in Hispanics (rate 0.444, CI 0.187-0.873), and 256 in Whites (rate 0.322, CI 0.284-0.365). 97 cases of NPC were recorded in the Alaska Native Tumor Registry (rate 6.590, CI 5.262-8.128). Twelve cases of EBV-positive NPC were identified in our archives (11 M, 1F, age range 15-61 years). Specimens were from 4 Native Americans (33%), 1 Hispanic (8%), 5 Whites (42%), and 2 Asians (17%). Age at presentation did not vary among subgroups.

Conclusions: New Mexican Natives have higher rates of NPC than New Mexican Hispanics and Whites. However, their rates are lower than Natives of the Pacific Northwest and Alaska. Factors that influence the development of NPC that may contribute to the lower prevalence include cigarette smoking rate, food preparation methods, and HLA subtype. Further, SEER data does not discriminate Navajo and Apache from other Native groups in New Mexico, who are not Athabaskan. Rates among the Navajo and Apache may ultimately prove to be higher.

1294 Mucoacinar Carcinoma: A Rare Intercalated Duct/Acinar Variant of Mucoepidermoid Carcinoma, Hybrid Tumor, or Distinct Entity?

Manish M Bundele, Ilan Weinreb, Bin Xu, Simon Chiosea, William Faquin, Dora Dias-Santagata, Raja R Seethala. Tan Tock Seng Hospital, SG, Singapore; University of Pittsburgh Medical Centre, Pittsburgh, PA; Massachusetts General Hospital, Boston, MA; University Health Network, Toronto, Canada; Sunnybrook Health Sciences Centre, Toronto, Canada.

Background: Mucoepidermoid carcinoma (MEC) is thought to recapitulate an excretory duct phenotype. However, occasional expression of intercalated duct/acinar markers (SOX-10 and DOG-1), suggest that this is not consistent. We now report 5 MEC that demonstrate serous acinar differentiation, further defying this canonical assumption.

Design: Clinicopathologic parameters for five MEC with serous acinar differentiation were reviewed. Tumors were graded using a modification of the Brandwein scheme (PMID: 20588178). Histochemical stains for Periodic acid Schiff after diastase (PAS-D) and immunohistochemical stains for SOX 10 and DOG1 were performed.

Break-apart fluorescence in situ hybridization (FISH) for *MAML2* rearrangements was performed on all cases (PMID: 22833306). Two cases (Cases 1 and 5) were tested using anchored multiplex PCR (AMP) and targeted next generation sequencing (MiSeq, Illumina San Diego CA) (PMID: 25384085) with a rearrangement panel targeting 52 genes including *MAML2* (exons 2-4).

Results: Clinicopathologic features are summarized below -

Cases	Age(yr)	Sex	Salivary gland site	Size(cm)	Grade
Case 1	23	F	Parotid	4.5	Low
Case 2	70	F	Parotid	1.3	Intermediate
Case 3	52	F	Parotid	2.0	Intermediate
Case 4	54	M	Submandibular	0.9	Intermediate
Case 5	72	M	Parotid	2.0	Low

All cases demonstrated prominent clear cell morphology and serous acinar differentiation (figure 1A). PAS-D (3/3), SOX-10 (4/4) (figure 1B), and DOG1 (5/5) (figure 1C) were positive in all tested cases. *MAML2* FISH was positive in all cases (figure 1D), in both acinar and mucoepidermoid components. Two cases tested by next generation sequencing showed standard *CRTC1-MAML2* fusions.

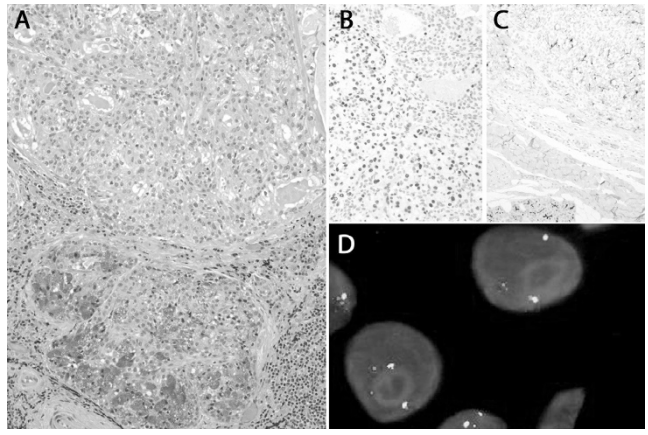

Conclusions: MEC with acinar differentiation or "mucoacinar" carcinomas represent a "distal" acinar variant morphology in MEC, rather than a distinct entity or collision tumor. The acinar differentiation and SOX-10/DOG-1 reactivity may thus be a diagnostic pitfall.

1295 Identification of Novel Gene Fusion EWSR1-CREM in Hyalinizing Clear Cell Carcinoma (HCCC) by Anchored Multiplex Polymerase Chain Reaction

Erin Chapman, Angela Goytain, Malcolm Hayes, Wei Xiong, Alena Skalova, Josh Haimes, Brian Kudlow, Cheng-Han Lee, Tony Ng. Vancouver General Hospital, Vancouver, BC, Canada; B.C. Cancer Agency, Vancouver, BC, Canada; St. Paul's Hospital, Vancouver, BC, Canada; Charles University, Pilsen, Czech Republic; ArcherDx, Inc., Boulder, CO; University of British Columbia, Vancouver, BC, Canada.

Background: EWSR1-CREB-family gene fusions are described in diverse neoplasms, including the characteristic EWSR1-ATF1 fusion in HCCC. Anchored multiplex polymerase chain reaction (AMP) is a next-generation sequencing-based technique in which novel gene fusions can be identified following PCR-based amplification that targets a panel of genes commonly involved in oncogenic fusions; one set of primers

target one partner gene, while the other partner is identified through next-generation sequencing agnostic to the identity of the other partner. We describe a novel gene fusion, EWSR1-CREM, identified in a case of HCCC using AMP.
Design: The patient was a 68 year old female with a base of tongue mass. Clear cell morphology, presence of mucin, and the immunoprofile raised a differential diagnosis of HCCC versus a mucoepidermoid carcinoma. EWSR1 and ATF1 FISH were performed during the initial diagnostic work-up. AMP was performed on this case with the goal of identifying the hidden fusion partner (Archer(R) Sarcoma FusionPlex(R) kit). Further testing included RT-PCR.
Results: Initial FISH showed the presence of an EWSR1 rearrangement but absence of an ATF1 rearrangement. AMP demonstrated a novel EWSR1-CREM fusion, with the fusion junction between EWSR1 exon 13 and CREM exon 5. This finding is biologically justified as CREM is a recognized paralog of ATF1, with both belonging to the CREB family of transcription factors.
Conclusions: We describe a case of HCCC demonstrating that CREM can replace ATF1 as the EWSR1 fusion partner. EWSR1-CREM fusions have not been previously reported in HCCC and have only rarely been reported in other tumours. We also show that a targeted next-generation sequencing-based assay such as AMP has the capability of discovering novel or unexpected fusion gene variants, and has clinical utility in the pathological classification of fusion gene-associated tumors with variable partner genes.

1296 Expression Pattern of Trk Proteins in Head and Neck Squamous Carcinoma and Its Prognostic Significance

Yoon Ah Cho, Ji Myung Chung, Eun Kyung Kim, Su Jin Heo, Byoung Chul Cho, Hye Ryun Kim, Sun Och Yoon. Yonsei University College of Medicine, Seoul, Republic of Korea.

Background: Treatment of head and neck squamous cell carcinomas (HNSCC) are challenging due to loco-regional recurrences and metastasis. Previous studies revealed that Tropomyosin-related kinase B (TrkB) is overexpressed in HNSCC. However, the relationship between HNSCC and subtypes of Trk proteins is not robustly studied. In this study, we try to evaluate expression of all subtypes of Trk proteins and its clinic-pathological significance.
Design: A total of 396 radically resected HNSCC cases were used for tissue microarray construction. Immunohistochemistry was performed for TrkA, TrkB, pan-Trk (TrkA+B+C) and evaluated through H-score analysis (0-300 scale). The cutoff for high Trk expression was determined at the mean value of H-scores.
Results: Oropharyngeal SCC revealed relatively higher expression of pan-Trk and TrkA ($P<0.05$). Expression of pan-Trk and TrkA was higher in p16-positive HNSCC than p16-negative cases ($P<0.001$). Expression of pan-Trk was higher in HNSCCs with lymphovascular invasion ($P<0.001$) , perineural invasion ($P=0.023$), more advanced pT ($P<0.001$), and more advanced pN stage ($P<0.001$) than cases without such factors. In patients of completely resected (R0 resection) oropharyngeal SCC, high TrkA expression was related to superior overall survival rate ($P=0.044$). In patients of oral cavity SCC with R0 resection, high pan-Trk was related to inferior overall survival rate ($P<0.001$). TrkB expression revealed no association with variable clinico-pathologic factors or patient prognosis.
Conclusions: Expression pattern of pan-Trk and TrkA was different according to anatomical sites and HPV infection status. High expression of pan-Trk may be related to poor prognosis, especially in oral cavity SCC while high TrkA expression may be related to favorable prognosis, especially in oropharyngeal SCC. Although further evaluation about implications of TrkC is necessary, Trk expression should be considered in the context of anatomical sites and each Trk subtype.

1297 Comprehensive Genomic Profiling of Salivary Gland Myoepithelial Carcinoma

Siddhartha Dalvi, Julia A Elvin, Jo-Anne Vergilio, James Suh, Shakti H Ramkissoon, Kai Wang, Daniel Bowles, Hilary Somerset, Siraj M Ali, Alexa Schrock, David Fabrizio, Garrett Frampton, Vincent Miller, Philip Stephens, Laurie M Gay, Jeffrey Ross. Albany Med Col, Albany, NY; Foundation Med, Boston, MA; Univers of Colorado, Denver, CO.

Background: Myoepithelial carcinomas (MyC) of salivary glands (SG) are typically low-grade malignancies that can arise de novo or in the background of a pre-existing pleomorphic adenoma (CPA). On occasion, MyC can present or progress into loco-regionally advanced and/or metastatic disease.
Design: DNA was extracted from 40 uμ of FFPE sections from 24 relapsed and metastatic MyC. Comprehensive genomic profiling (CGP) was performed using a hybrid-capture, adaptor ligation based next generation sequencing assay to a mean coverage depth of >712X. Tumor mutational burden (TMB) was calculated from a minimum of 1.11 Mb of sequenced DNA and reported as mutations/Mb. The results were analyzed for all classes of genomic alterations (GA), including base substitutions (sub), insertions and deletions (short variants), fusions, and copy number changes including amplifications (amp) and homozygous deletions.
Results: 21 (87.5%) of MyC arose de novo and 3 (12.5%) presented as carcinoma ex pleomorphic adenoma. 14 (58%) MyC patients were male and 10 (42%) female with a mean age of 61.3 years (range 26 to 83 years). 4 (18%), 6 (25%) and 14 (58%)MyC were well, moderately and poorly differentiated. At the time of CGP, 10 (42%) MyC were stage III and 14 (58%) were stage IV. Sequencing was performed on the primary and metastatic sample in an equal number of cases (12 each). Of 22 cases where the primary site was known 16 (73%) arose in the parotid SG, 1 (5%) in the submandibular SG and 5 (22%) from accessory SG. The 24 MyC featured 2.3 GA/case with the most frequent clinically relevant GA (CRGA) involving *RICTOR* amp and *PIK3CA* sub (13%); *PTCH1* and *PDGFRB* sub (8% each) and *NF1* and *BRCA2* sub (4% each). There were no ERBB2 GA. The most frequent non-actionable GA were *CDKN2A* loss (25%), *CDKN2B* loss and *HRAS* sub (21% each), *TERT*, *MYC*, *TP53* and *NOTCH1* subs (13% each).2 (8%) MyC featured TMB > 20 mut/Mb and 22 (92%) featured TMB < 10 mut/Mb. No MyC cases had MSI-high status.
Conclusions: Clinically advanced MyC are similar to the usually less aggressive SG tumors, adenoid cystic and acinic cell carcinomas in having low GA/tumor, low *TP53* mutation frequency, low TMB and general paucity of CRGA when compared to the usually more aggressive adenocarcinomas which may feature alterations in *ERBB2* and other pathways. However, the findings of CRGA in *RICTOR, PTCH1*, *NF1* and *BRCA2* and the presence of high TMB in a subset of MyC cases encourages continued use of CGP to search for targeted and immunotherapies for this rare type of progressive head and neck cancer.

1298 Genomic Profiling of the Two Closely Related "cousins" Acinic Cell Carcinoma and Mammary Analog Secretory Carcinoma of Salivary Glands Reveals Novel *NCOA4-RET* Fusion in Mammary Analog Secretory Carcinoma

Snjezana Dogan, Ryma Benayed, Hui Chen, Maria E Arcila, Michael F Berger, Nora Katabi. Memorial Sloan Kettering Cancer Center, New York, NY.

Background: Acinic cell carcinoma (AciCC) is a rare malignant salivary gland neoplasm that is genetically largely undefined. Mammary analog secretory carcinoma (MASC), a recently described entity previously classified as AciCC is characterized by *ETV6-NTRK3* fusion. However, a minor proportion of tumors morphologically compatible with MASC are negative for *ETV6* rearrangement suggesting the presence of other driver genetic alterations. Here, we used a broad genomic analysis to examine the differences between the two morphologically close tumor entities.
Design: Genomic profiling was performed on 22 tumors including 15 (68.2%) AciCCs, 6 MASCs (27.3%), and one (4.5%) high grade carcinoma with features of both, AciCC and MASC (AciCC/MASC). A hybridization exon-capture next-generation sequencing assay (MSK-IMPACT™) interrogating genomic alterations in 341 key cancer-associated genes was preformed on 13 AciCCs and 2 MASCs. An RNA based Archer's Anchored Multiplex PCR™ using the FusionPlex™ 35 gene panel (Archer™ fusion assay) was performed in 7 additional cases including 4 MASCs, 2 AciCCs and one AciCC/MASC. One MASC was tested by both assays.
Results: Overall 16 genomic alterations (GA) with an average of 1.2 GA per case were detected in 13 AciCCs by MSK-IMPACT™ including truncating events or whole gene deletions in tumor suppressor genes *NF1, BAP1,* and *PTEN,* mutations in *XPO1, NOTCH4, GRIN2A, ARID2, SMARCB1, ATM, PAX5,* and amplifications in *KLF6, MCL1* and *PIK3CD.* No GA was detected in 6 (46.2%) AciCCs. No fusion gene was detected in 3 AciCCs and one AciCC/MASC byArcher™ fusion assay. Among 4 tumors morphologically and immunophenotypically compatible with MASC that were tested by Archer™ fusion assay only, one showed an *ETV6-NTRK3* fusion, another a *NCOA4-RET* fusion, and 2 cases were fusion negative. One MASC profiled by both assays was fusion negative and showed multiple copy number alterations including *CDKN2A* deletion, and amplifications of *CCND1, SOX2, NTRK2, CTNNB1, PAX5, TNFAIP3, FLT3, MYB, DNMT3A, MPL and SOCS1*.
Conclusions: AciCC is characterized by a relatively 'quiet' genome. A subset of *ETV6-NTRK3* negative MASCs harbor *NCOA4-RET* fusion possibly rendering these tumors amenable to targeted therapy with RET inhibitors. A more comprehensive genomic profiling of AciCCs and fusion negative MASCs would be necessary to identify potentially novel driver mutations.

1299 RNA In Situ Hybridization (ISH) for 18 High Risk Human Papilloma Viruses (HPV) in Squamous Cell Carcinoma (SCC) of the Head and Neck: Comparison with p16 Immunohistochemistry (IHC)

Bradley Drumheller, Cynthia Cohen, Diane Lawson, Momin T Siddiqui. Emory University Hospital, Atlanta, GA.

Background: The relationship between high risk HPV infection and subsets of head and neck SCC is well established. Detection is important in deciding treatment, as HPV-related SCCs respond better to therapy. The gold standard is identifying the viral oncogene mRNA (E6/E7) by reverse-transcriptase PCR (RT-PCR) in fresh tissue, indicating active infection. However, this expensive and technically demanding approach limits its clinical application. IHC staining of formalin fixed paraffin embedded (FFPE) tissue for the indirect marker p16, and HPV-DNA is more practical for most laboratories. p16 IHC has limited specificity and can be challenging to interpret. HPV-DNA ISH has limited sensitivity. The RNAscope HPV-test is a novel RNA ISH which strongly stains transcripts of E6/E7 mRNA in FFPE tissue with the potential for clinical use.
Design: De-identified FFPE samples from 27 patients with SCC of the oral cavity and pharynx (2015-2016) were stained using RNA ISH to detect high-risk HPV E6-E7 mRNA and compared to p16 IHC (Ventana RTU). The RNA ISH used the RNAscope (Leica BioSystems, Buffalo Grove, IL), the Bond III autostainer (Leica), and RNAscope® 2.5 LS Probe - HPV-HR18 (high risk pool of 18 individual HPV probes: HPV 16, 18, 26, 31, 33, 35, 39, 45, 51, 52, 53, 56, 58, 59, 66, 68, 73, and 82; Advanced Cell Diagnostics, Newark, CA), as well as a negative (Dap B) and positive probe (PP1B for RNA). Two pathologists reviewed and graded the RNA ISH stained-slides and reached a consensus on all interpretations.
Results: RNAscope HPV test detected 100% (21/21) of the p16 IHC positive samples. It detected 50% of the p16 IHC negative samples (3/6). These three RNA ISH positive samples had rare positivity, read as <5%. All other positive samples had >10% positivity. All of the RNA ISH negative samples were p16 IHC negative (3/3). Overall, the two results were concordant in 88.9% of the samples.

	P16+	P16 -
RNA ISH +	21	3
RNA ISH -	0	3

Sensitivity	100%
Specificity	50%
Positive Predictive Value	87.5%
Negative Predictive Value	100%
Accuracy	88.9%

Conclusions: Directly detecting RNA products is an excellent marker for active HPV infectivity. This method stains cells very strongly with minimal background noise, leading to increased detection. The rare cells that stained <5% with RNA ISH in the three samples are probably at an undetectable threshold for p16 IHC.

1300 Subsets of Epithelial Myoepithelial Carcinoma Defined by Morphologic Evidence of Pleomorphic Adenoma, PLAG1 or HMGA2 Rearrangements, and Genetic Alterations

Soufiane El Hallani, Diana Bell, Isabel Fonseca, Adel Assaad, Raja R Seethala, Lester DR Thompson, Simon Chiosea. University of Pittsburgh, Pittsburgh, PA; MD Anderson, Houston, TX; Instituto Português De Oncologia De Francisco Gentil, Lisboa, Portugal; SCPMG, Woodland Hills, CA; Virginia Mason Hospital, Seattle, WA.

Background: Histogenetic classification of epithelial myoepithelial carcinoma (EMCA) would account for *de novo* tumors and those with morphologic or molecular (*pleomorphic adenoma gene 1 [PLAG1*], *high-mobility group AT hook 2 [HMGA2*] rearrangement, amplification) evidence of pleomorphic adenoma (PA).

Design: EMCAs (n=39) were reviewed for morphologic evidence of PA. High grade transformation (HGT) was defined by the presence of necrosis. *PLAG1* and *HMGA2* alterations were detected by fluorescence in situ hybridization (FISH). EMCAs with intact *PLAG1* and *HMGA2* (n=11) were tested for other fusions, including *fibroblast growth factor receptor 1 (FGFR1)-PLAG1*, as previously described (PMID: 26747586). Twenty-three tumors were also analyzed for mutations and copy number variations in 50 cancer-related genes (PMID: 27379604).

Results: Based on combined morphologic and molecular evidence of PA, 4 subsets of EMCA emerged: 1) carcinomas with morphologic evidence of PA but intact *PLAG1* and *HMGA2* (n=10); 2) carcinomas with *PLAG1* fusion (n=9); 3) *HMGA2* alteration (n=9, including 3 cases without morphologic evidence of PA); and 4) de novo carcinomas, without morphologic or molecular evidence of PA (n=11). Two cases with intrachromosomal *FGFR1-PLAG1* fusion were identified by RNA fusion panel only (*PLAG1* FISH was negative). Disease-free survival and clinicopathologic parameters did not differ for the subsets defined above. The relationship between the 4 subgroups, presence of HGT, and molecular findings are summarized in Figure 1.

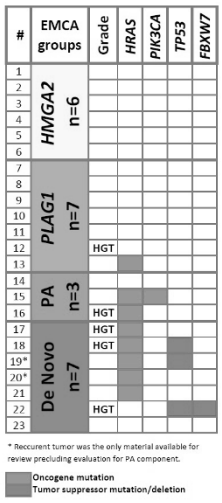

HRAS (5 of 7 vs 3 of 16 tumors; p=0.01) and *TP53* alteration (3 of 7 vs 0 of 16 tumors; p<0.01) were observed predominantly in de novo carcinomas.

Conclusions: Most EMCAs are ex PA (28/39, 72%). The genetic profile of EMCAs varies with the absence or presence of pre-existing PA and its molecular signature. *PLAG1* FISH underestimates the prevalence of *FGFR1-PLAG1* fusion by 18% (2/11). The de novo EMCAs more commonly harbor *HRAS*, *TP53*, and/or *FBXW7* alterations.

1301 Melan-A Expression in Olfactory Neuroblastoma

Amelia Fierro-Fine, Robert Robinson, Anthony Snow. University of Iowa, Iowa City, IA.

Background: Olfactory neuroblastoma is a rare tumor of the sinonasal tract of neuroectodermal origin representing nearly 6% of nasal and paranasal sinus tumors. The cell of origin is thought to be a reserve neuroepithelial cell of the sinonasal tract with neuro-endocrine capabilities including production of neurosecretory granules. Some olfactory neuroblastomas have melanin or a melanin-like pigment which may confound the diagnosis with sinonasal melanoma. Our group encountered a small biopsy which showed few distinguishing morphologic features and strong positivity for Melan-A (MART-1) that ultimately proved to be an olfactory neuroblastoma. No significant literature documenting Melan-A positivity in olfactory neuroblastoma was available for comparison. Melan-A IHC is examined in olfactory neuroblastoma to determine its usefulness in distinguishing olfactory neuroblastoma from sinonasal melanoma or to provide evidence to avoid its use.

Design: Formalin fixed paraffin embedded olfactory neuroblastoma specimens from 25 patients were identified from our case files between 1997 and 2015. The FFPE blocks were stained with anti-human Melan-A monoclonal mouse antibody (Dako, Clone A103) at a 1:25 dilution, and the staining strength and pattern were evaluated by two pathologists.

Results: 4 of 25 olfactory neuroblastomas showed diffuse weak (1+) cytoplasmic immunohistochemical positivity for Melan-A while 2 cases showed moderate (2+) patchy cytoplasmic staining, 1 case showed diffuse strong (3+) cytoplasmic staining, and 1 case (the index case) showed diffuse strong (3+) cytoplasmic staining and nuclear signal.

Conclusions: 28% of cases of olfactory neuroblastoma demonstrated immunohistochemical positivity for Melan-A. All showed either diffuse and/or strong signal. It has not been determined whether the signal is from Melan-A produced by the tumor, or cross reactivity with similar steroid epitopes in some olfactory neuroblastomas. Cross reactivity is favored as the character of cytoplasmic staining is finer than that commonly observed in melanoma and nuclear signal was observed in some cases. Similar examples of probable cross reactivity have been established in adrenocortical tumors, granulosa cell tumors, and leydig cell tumors particularly with clone A103. Interpretation of Melan-A positivity should be approached with caution in the context of small biopsies from the sinonasal mucosa in which melanoma and olfactory neuroblastoma enter the same differential diagnosis. Additional immunohistochemical studies and correlation with morphologic and clinical data are required to reach a correct diagnosis.

1302 Precision HPV Mapping Indicates That Oropharyngeal Squamous Cell Carcinomas Arising in Non-Tonsillar Sites Are Not HPV-Related

Elise Gelwan, Ian-James Malm, Carole Fakhry, Justin A Bishop, William H Westra. The Johns Hopkins Hospital, Baltimore, MD.

Background: The oral cavity and oropharynx form one continuous chamber lined by an uninterrupted stratified squamous epithelium. Accordingly, the oral cavity and oropharynx have historically been viewed as a single compartment of the head and neck. The practice of combining these sites has recently been revised, largely owing to the observation that human papillomavirus (HPV)-driven carcinogenesis preferentially targets the oropharynx but not the oral cavity: HPV is detected in over 70% of oropharyngeal squamous cell carcinomas (SqCC) but in less than 5% of oral SqCCs. The purpose of this study was to determine whether HPV is evenly distributed across SqCCs of the oropharynx including those sites that do not harbor tonsillar tissues (e.g. soft palate).

Design: A search of the medical records identified 30 primary SqCCs of the soft palate (n=29) and posterior pharyngeal wall (n=1). These were evaluated with p16 immunohistochemistry. P16 positive tumors were further evaluated with high risk HPV RNA in situ hybridization (RISH). Those tumors that were P16 positive (>70% staining) and HPV RISH positive were considered to be HPV positive.

Results: 18 (60%) of the patients were male. The patients ranged in age from 46 to 81 years (mean, 60). 50% were Caucasian, 43% were African American, 3% were Asian, and 3% were Hispanic. 83% of patients were current or former smokers (average pack-year history, 52). 80% of patients reported a history of alcohol use. By routine histology, 91% of the SqCCs showed surface dysplasia, and 88% were keratinizing or partially keratinizing. Only 1 tumor was p16 positive, but it was HPV negative by HPV RISH. In effect, none of the SqCCs were HPV related.

Conclusions: HPV is not frequently detected in SqCCs of the soft palate. Based on comprehensive profiling (e.g. demographic, risk factors, histologic, HPV status), soft palate SqCCs more closely resemble those arising in the oral cavity than those arising in the lingual and palatine tonsils of the oropharynx. This observation: 1) supports the position that oncogenic HPV specifically targets the tonsillar crypt epithelium and not the squamous epithelium lining the surface of the oropharynx; 2) prompts consideration of further anatomic subtyping of the oropharynx based on the presence or absence of tonsillar tissue; 3) challenges indiscriminant HPV testing of all oropharyngeal SqCCs irrespective of anatomic subsite; and 4) suggests that rates of HPV in oropharyngeal SqCCs may vary depending on the anatomic distribution of the tumors within the oropharynx.

1303 SOX10 and GATA3 Expression and Clinical Utility in Adenoid Cystic Carcinoma and Polymorphous Low Grade Adenocarcinoma of the Head and Neck

Ariana B Geromes, Rebecca Chernock, Katherine Kimmelshue, James Lewis, Kim Ely. Vanderbilt University Medical Center, Nashville, TN; Washington University School of Medicine, St. Louis, MO.

Background: Discriminating between adenoid cystic carcinoma (AdCC) and polymorphous low grade adenocarcinoma (PLGA) can be difficult on small biopsy and cytologic specimens. SOX10 expression has been noted in myoepithelial cells of the salivary gland and prior studies have reported its utility in delineating two distinct subtypes of salivary gland tumors: acinic cell, adenoid cystic, epithelial myoepthelial carcinoma, myoepithelioma, and pleomorphic adenoma are positive, while salivary duct carcinoma and mucoepidermoid carcinoma are negative. There is scant data regarding SOX10 expression in PLGA. GATA3 reactivity can be seen in many types of salivary gland tumors, particularly mammary analogue secretory carcinoma and salivary duct carcinoma while AdCC does not express this marker. There is minimal data regarding GATA3 expression in PLGA, with a prior study reporting no staining in a small series of cases. We aimed to document GATA3 and SOX10 expression in PLGA and AdCC and determine whether these markers are of diagnostic utility in delineating these two entities.

Design: From electronic searches of department databases, we gathered 25 PLGA and 25 AdCC cases from resection specimens taken from 1994-2015. Diagnoses were confirmed by at least 1 study pathologist. Immunohistochemical analyses for GATA3 and SOX10 were performed on whole tumor sections. Staining was scored on a 0-16 scale (intensity of staining [1-4] multiplied by extent of staining [0-4]). A score of ≥ 3 was considered positive.
Results: SOX10 was expressed in 100% of PLGA and AdCC in a strong and diffuse manner with scores ≥ 8 in 100% of PLGA and 88% of AdCC. GATA3 was expressed in 45% (10/25) of AdCC. When positive, GATA3 staining in AdCC was dim and patchy with scores < 8 in 80% of cases. A subset of PLGA cases, 20% (5/25), showed focal but strong GATA3 reactivity specifically in areas with ductal differentiation. The remaining PLGA cases were negative.
Conclusions: Our study documents the expression of GATA3 and SOX10 in whole sections of PLGA and AdCC. SOX10 stains both AdCC and PLGA in a strong, diffuse fashion. GATA3 stains less than 50% of AdCC in a patchy, dim manner, while a subset of PLGA with ductal differentiation show focal, strong staining. Though interesting, this is not likely to be of clinical utility. In conclusion, SOX10 and GATA3 immunohistochemical stains do not appear useful in differentiating between AdCC and PLGA.

1304 PEComas of the Head and Neck: Diagnostic Challenges of a Rare Tumor with Variable Immunophenotype and Behavior

Abigail L Goodman, Kelly R Magliocca, Christopher C Griffith. Emory University, Atlanta, GA.

Background: Perivascular epithelioid cell tumors (PEComas) are mesenchymal tumors occurring in a variety of sites but exceptionally rare in the head and neck (H&N). These tumors represent a significant diagnostic challenge and criteria for predicting malignancy are not well studied. Here we review our experience with H&N PEComas focusing on immunophenotype and morphologic features.
Design: A retrospective institutional archival study of PEComas of the H&N excluding cutaneous tumors was performed. Demographic information including patient age, sex, potential risk factors, anatomic location, prior imaging studies, treatment and clinical follow-up were abstracted. H&E and immunostained slides were reviewed for mitotic activity, necrosis, nuclear grade, and immunophenotype.
Results: Three PEComas were identified, all of which showed epithelioid morphology and had immunophenotypic evidence of melanocytic differentiation but negative S100 reactivity. One case was negative for muscle markers (smooth muscle actin and desmin). Two cases were classified as malignant based on high nuclear grade, cellularity, and mitotic rate ≥ 1/50 HPF. The base of tongue tumor can be seen in figure 1 with Melan A and MITF reactivity. All patients were treated with complete tumor resection and malignant tumors received adjuvant radiotherapy. No recurrence or metastasis has been reported for either malignant tumor at 5 and 17 months.

Age/ Sex	Location	Size (cm)	Predicted Behavior	HMB-45	Melan A	MITF	Actin
55/M	Base of Tongue	3.5	Malignant	-	+	+	-
48/F	Sinus	3.0	Malignant	+	Rare +	-	+
8/M	Anterior nasal	1.2	Benign	-	-	+	+

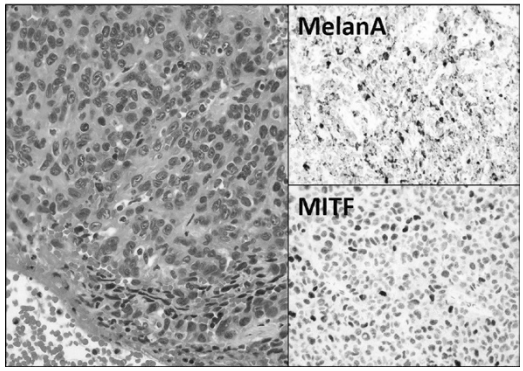

Conclusions: This series includes the first reported case of PEComa of the base of tongue. These cases demonstrate the challenge of diagnosing PEComa in unusual sites and the importance of using multiple melanocytic markers including HMB-45, Melan A, and MITF. Although 2/3 were designated malignant based on histologic features there has been no recurrence/metastases but follow-up is limited.

1305 A First Look at the Genomic Landscape of Non-Metastatic Cutaneous Squamous Cell Carcinoma

Ruta Gupta, Catherine Zilberg, Matthew Lee, Bruce Ashford, Jonathan Clark, Marie Ranson, Bing Yu, Sandra O'Toole. The Chris O'Brien Lifehouse (LH), Camperdown, New South Wales, Australia; Royal Prince Alfred Hospital (RPAH), Camperdown, New South Wales, Australia; Illawarra Health and Medical Research Institute (IHMRI), Wollongong, New South Wales, Australia.

Background: Cutaneous Squamous Cell Carcinoma is the second most prevalent malignancy and most-frequently occurs in the head and neck (HNcSCC). Treatment of locally advanced or metastatic disease is associated with significant functional morbidity and disfigurement. There is limited understanding of the underlying genetic mechanisms in high risk HNcSCC.
Design: Targeted sequencing of 48 clinically relevant genes was performed on DNA extracted from formalin fixed and paraffin embedded non-metastatic high risk HNcSCCs. SIFT and PolyPhen output, existing genomic databases, functional and structural implications of detected mutations were considered in significance determination. Observed genetic alterations were compared with data reported for physiologically normal skin and metastatic cSCC. Associations with clinicopathologic characteristics were evaluated.
Results: We identified somatic alterations in 44 cancer-associated genes. Missense variants comprised 72% of the mutations. Samples showed variability in number and type of genes affected. *TP53* was mutated in all samples, *APC, ATM, ERBB4, GNAQ, PTEN*, *PDGFRA, ABL1, FGFR3, KIT, NRAS, RB1 and VHL* were altered in at least 50% of samples. Tumor suppressor alterations were most common in this cohort. The cell cycle/apoptosis pathway, mTOR, MAPK and PI3K pathways were most commonly altered. All samples with alterations in *FGFR2* had peri-neural invasion. There were far fewer alterations in *NOTCH* genes and *CDKN2A* compared with metastatic cSCC. Somatic mutations associated with susceptibility to combined EGFR inhibitors, mTOR inhibitors, broad-spectrum tyrosine kinase inhibitors and DNA demethylating agents were identified.

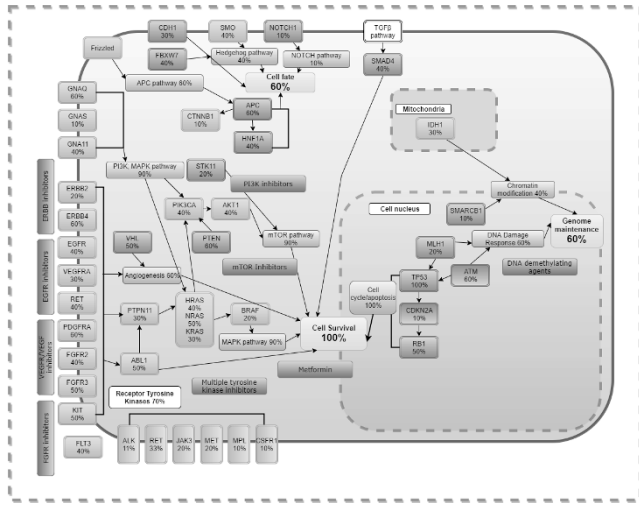

Conclusions: The study provides an initial insight into the genomic landscape of non-metastatic, high risk HNcSCC and identifies targeted therapies that may merit further investigation in HNcSCC. It highlights the association of certain alterations such as *FGFR2, NOTCH* and *CDKN2A* that may play roles in local or distant cancer progression.

1306 Odontogenic Myxoma: Review of Histopathologic, Immunocytochemical and Ultrastructural Features

Mohammad Haeri, H Wu, C Finch, D Citron, O Roncal, John Hicks. Baylor College of Medicine & Texas Children's Hospital, Houston, TX.

Background: Odontogenic myxomas arise from odontogenic ectomesenchyme and involve the mandible and maxilla. Most are located in the mandible (two-thirds). There is a wide age range, with an average age of 25 to 30 years. The typical tumor is asymptomtic with painless jaw expansion, and found incidentally during dental examination. Diagnostic imaging may reveal a unilocular, multilocular or soap bubble lesion, displacing and/or resorbing teeth. The tumor is not encapsulated, infiltrates bone and may require aggressive curettage.
Design: Study population consisted of 6 males and 5 females (age range 11-62 years) with 6 mandibular and 5 maxillary tumors. The tumors ranged in size from 1.5 cm to massive involvement of the entire maxilla with extension to orbital floors. Tissue was available for routine, immunocytochemical (vimentin, MSA, SMA, S100 protein) and electron microscopic examination.
Results: Gross examination demonstrated white to tan, gelatinous to mildly firm tumors with a mucinous character. The tumors were composed of stellate to ovoid to slightly spindled cells within abundant myxoid matrix with infrequent collagen fibers. One tumor showed malignant transformation from typical odontogenic myxoma to an odontogenic myxosarcoma (low grade myxofibrosarcoma). Tumor cells expressed vimentin diffusely, focal SMA and focal MSA, and lacked S100 expression. Electron microscopy showed widely spaced cells with a mesenchymal character and scant cytoplasm. The tumor cells had adherent basal lamina material. The stroma was composed of ground substance with scant scattered collagen fibers. The odontogenic myxosarcoma had markedly increased cellularity, more elongated spindle cells in close proximity, decreased ground substance and increased collagen fibers.
Conclusions: Odontogenic myxomas may be confused with other myxoid jaw neoplasms, such as myxoid nerve sheath tumor, chondromyxoid fibroma, myxoid fibrosarcoma and other myxosarcomas, especially when small biopsies are taken. Hyperplastic dental follicle with myxoid change, a dental papilla from a developing tooth or nasal polyp may be mistaken for an odontogenic myxoma. Review of diagnostic imaging of a jaw mass and clinical history are important in providing an accurate diagnosis and guiding appropriate surgical management.

1307 Salivary Duct Carcinoma and Invasive Ductal Carcinoma of the Breast: A Comparative Immunohistochemical Study

Jalal B Jalaly, Souzan Sanati, Rebecca Chernock, Samir K El-Mofty. Washington University, Saint Louis, MO.

Background: Salivary duct carcinoma (SDC) is a high-grade salivary gland malignancy with great morphological resemblance to invasive ductal carcinoma (IDC) of the breast. SDC is more common in men, but according to some reports they are more aggressive in women. When patients present with metastatic disease, the differential diagnosis may include both IDC and SDC. Rarely, female patients may have a past history of both SDC and IDC and may present with distant metastasis. Moreover, metastasis of SDC to the breast and IDC to the salivary (parotid) gland has been reported as well. Our aim is to develop an immunohistochemical panel that reliably distinguishes SDC from IDC.

Design: All primary SDCs were included (1989-2016). Metastatic SDCs were included only if the primary tumor was a known SDC in the absence of available tissue from the primary site. Resection specimens from recent (2016), treatment naïve IDCs were included if they morphologically resemble SDC and were of grade 2 or 3 by Nottingham grade. All tumors were stained with androgen receptor (AR), estrogen receptor-alpha (ER-α), progesterone receptor (PR), HER-2, CK5/6, p63, and beta-catenin. Chi-square test was used for statistical analysis.

Results: SDCs from 23 patients were included in the study (73.9% males) with an average age of 60.7 years (range 47 to 79 years). There were 29 IDCs (15 grade 2 and 14 grade 3, mean patient age of 53.6 years). A minority of cases of both SDC and IDC reacted to CK5/6 and p63. Both tumors were AR and beta-catenin (membranous) positive in more than 90% of cells. The main disparity in their immunohistochemical profiles was a distinctly different reactivity to ER-α, PR and HER-2. While 27 IDCs (93.1%) reacted positively to ER-α and/or PR, the majority expressing both (88.9%) with a 3+ intensity, only 2 SDCs expressed ER-α (8.7%) and 2 others expressed PR (8.7%) with an intensity of 1-2+ (P value <0.05) . On the other hand, 17 SDC (74%) were positive for HER-2 while only 5 (17%) IDC were positive (P value <0.05). Table 1 shows the percent positive cases in both types of tumors.

Immunostain	IDC	SDC
ER-alpha	86.2%	8.7%
PR	89.7%	8.7%
HER-2	17.2%	73.9%
AR	93.1%	91.3%
p63	27.6%	26.1%
CK5/6	20.7%	39.1%
Beta-catenin (membranous)	96.6%	100%

Conclusions: ER-α, PR, and HER-2 may be helpful to distinguish SDC from IDC. Positive reactivity to ER-α, PR or both and negative HER-2 favors a diagnosis of IDC while ER-α, PR negative, HER-2 positive tumors are more likely SDC.

1308 Is Regional Lymph Nodes Metastasis of Head and Neck Paraganglioma a Sign of Aggressive Clinical Behavior? A Clinical/pathologic Review

Sara Javidiparsijani, Diana Lin, Vijaya B Reddy, Pincas Bitterman, Paolo Gattuso. RUSH University Hospital, Chicago, IL.

Background: Head and neck paraganglioma accounts for <1% of all head and neck tumors. It usually has benign clinical course; however, malignant paraganglioma can only be diagnosed by showing metastatic disease. We undertook a retrospective study to assess the clinical significance of regional lymph nodes metastases in head and neck paragangliomas.

Design: From 1993 to 2016, 63 primary head and neck paragangliomas were identified in our institution's pathology file. Patient clinical and histopathologic data were reviewed.

Results: Of 63 patients, 49 were female and 14 were male (mean age of 54 yrs, range24 -78). Locations included: carotid body- 30, glomus tympanicum- 13, glomus jugulare- 12, parapharyngeal space- 3, infratemporal fossa- 2, and 1 case each of larynx, skull base and pyriform sinus. 58 cases were classic and 5 were sclerosing variant. 32/63 cases (50%) had concurrent regional lymph node biopsies (1-29 lymph nodes). 4/32 (12%) showed metastatic paraganglioma (3 females, 1 male, mean age= 35), including 2 sclerosing variant cases. The primary locations were: 2 carotid body, 1 infratemporal fossa and 1 glomus tympanicum. There was no evidence of local recurrence or distant metastasis in the patients with positive lymph nodes with a follow up of up to 22 years (mean=12 years).

1/28 patient with negative lymph nodes developed lumbar spine metastasis 5 years later. 6/31 (19%) of patients without lymph node evaluation had local recurrence, most likely due to residual disease.

Conclusions: The incidence of lymph node metastasis was 12%.

Metastatic paraganglioma to regional lymph nodes may have an indolent clinical behavior, with disease free survival of up to 22 years.

40% of lymph node metastases were sclerosing variant indicating that this tumor may have a more aggressive clinical behavior.

1/59 (1.6%) , 28 patients with negative lymph nodes and 31 patients without lymph node sampling, developed distant metastasis.

Clinical factors associated with metastasis were young age (mean 35 years, p=0.02), female gender, and carotid body location, although the age is the only parameter that was statistically significant.

1309 HER2 Stain Scoring in Salivary Duct Carcinoma

Ming Jin, David W Cohen, Paul E Wakely. The Ohio State University Wexner Medical Center, Columbus, OH.

Background: Salivary duct carcinoma (SDC) is a rare malignancy of salivary gland. The clinical utility of HER2 in SDC remains unclear. HER2 over-expression in SDC by immunohistochemistry (IHC) has been reported as a wide range. Thus far, a standardized HER2 IHC scoring system (SS) for SDC does not exist. HER2 SS for breast cancer (BC) and gastric/ gastroesophageal junction adenocarcinoma (GEC) have been developed separately by randomized controlled trials. Major scoring differences between these two exist [BC 3+: strong circumferential/complete membrane staining>10%; GEC 3+: strong complete, basolateral, or lateral membrane staining>10% in resection; regardless % in biopsy]. Pathologists have been adopting the BC SS for SDC due to its morphological resemblance to BC. There is no well-designed study regarding the rationale for this approach. Our aim was to assess the rate of SDC HER2 over-expression and evaluate scoring concordance using both BC and GEC SS.

Design: A retrospective search was performed to identify SDC cases. HER2 IHC was scored by BC and GEC SS. Cases with score of ≥ 2, membrane staining completeness, and intratumoral heterogeneity (ITH, defined by 2 or more different HER2 scores with >10% of total tumor) were also evaluated.

Results: 59 SDC cases (43 primaries, 3 recurrences, 13 metastases; 54 tissue resections, 5 biopsies) from 45 patients (M:F = 2:1; mean age = 64) were included. HER2 IHC over-expression by BC SS (determined on the primary resection if the score was different in other specimens) was: negative (0/1+) 15/45 (33%), equivocal (2+) 11/45 (24%), and positive (3+) 19/45 (42%). 2/59 demonstrated scoring discordance by BC and GEC SS due to strong but incomplete membrane staining: one resection with 2+ by BC SS and 3+ by GEC SS; one biopsy with 2+ by BC SS, 3+ by GEC SS (corresponding resection 3+ by both SS). Of 41/59 with a score of ≥2, 6 showed focally incomplete membrane staining; 26 demonstrated ITH. Additionally, 2 cases with 1+ score displayed incomplete strong membrane staining, but the low percentage (5%) was not significant enough to change the final score.

Conclusions: In our series of 45 patients, HER2 overexpression by BC SS was seen in 42%. Strong incomplete membrane staining in SDC is uncommon, and mostly focal when present. Therefore, using HER2 BC SS appears to be appropriate for SDC. The presence of ITH in a substantial number of cases raises the concern that small biopsies may not be suitable for accurate scoring. Future HER2 testing by FISH on equivocal cases should establish the true gene amplification rate.

1310 Recurrent *IDH2* R172X Mutations Define Sinonasal Undifferentiated Carcinoma

Vickie Y Jo, Nicole G Chau, Jason L Hornick, Jeffrey F Krane, Lynette M Sholl. Brigham and Women's Hospital and Harvard Medical School, Boston, MA; Dana-Farber Cancer Institute and Harvard Medical School, Boston, MA.

Background: Sinonasal undifferentiated carcinoma (SNUC) is a rare aggressive malignant neoplasm that lacks well-established diagnostic criteria. SNUC is considered a diagnosis of exclusion once epithelial differentiation is identified and other entities have been excluded. The molecular pathogenetic basis for SNUC is unknown.

Design: 11 cases of SNUC diagnosed between 2007-2016 with available tissue were identified in the archives. Diagnoses were confirmed by expert review of H&E slides and immunohistochemical (IHC) studies. DNA was extracted from FFPE samples for next-generation sequencing of all coding regions and selected introns for ~300 cancer genes. Institutional head and neck cohorts (n=412) were reviewed to explore mutational frequencies across relevant diagnoses. IHC using a multispecific antibody for IDH1/2 (R132/172) mutant protein was performed on 6 cases.

Results: The patient group consisted of 6 men and 5 women, age range of 41-75 years (median 64). Tumor sites were nasal (5), nasopharynx (1) maxillary sinus (2), ethmoid sinus (2), sphenoid sinus (1). All SNUCs showed sheetlike or nested growth of medium-large cells with hyperchromatic vesicular nuclei, prominent nucleoli, and scant-to-moderate eosinophilic cytoplasm; necrosis and brisk mitotic activity were present. All tumors showed strong diffuse cytokeratin expression. Limited staining for p63/p40 (1/10), synaptophysin (2/10), chromogranin (3/9), and S-100 (2/9) was seen. Negative IHC included desmin (0/7), NUT (0/8), and EBER (0/6); INI1 (SMARCB1) was retained (7/7). Sequencing identified *IDH2* R172 mutations in 6 (55%) SNUCs: R172S (3), R172T (2), and R172M (1). By IDH1/2 IHC, 3/3 SNUCs with R172 mutations were positive; 3 wild-type cases were negative. Genetic alterations in *IDH2* wild-type cases included 1 tumor with a *SMARCA4* splice variant (with confirmed loss of SMARCA4 expression by IHC) and 1 case with a *NOTCH1* PEST domain mutation. Review of sequencing data for the head and neck cohorts confirmed absent *IDH* activating mutations in other tumor types.

Conclusions: SNUCs are a genomically heterogeneous class of tumors; however, our findings suggest that a limited number of pathway alterations lead to a similar cancer phenotype. *IDH2* R172X mutations are a dominant finding in SNUCs and are specific to SNUCs in the differential diagnosis with other malignant neoplasms of the head and neck. The identification of frequent *IDH2* mutations in SNUC has significant diagnostic and therapeutic implications.

1311 Papillary Cystic Variant of Acinic Cell Carcinoma Masquerading as Mammary Analogue Secretory Carcinoma of Salivary Gland

Shubhada Kane, Nikita S Oza, Asawari Patil, Munita Bal, Trupti Pai, Ruta Gupta. Tata Memorial Hospital Parel, Mumbai, Maharashtra, India; Gravan Institute of Medical Research, Sydney, Australia.

Background: MASC is recently recognized tumor of salivary gland with characteristic t (12; 15) (q13; q25) translocation with ETV6-NTRK3 fusion product. The close differential diagnosis is Acinic cell carcinoma (AciCC). Before the advent of MASC,

majority of cases showing predominant papillary pattern were termed as Papillary Cystic Variant of AciCC. It is now possible to distinguish these entities from one another with molecular testing.The objective of our study is to establish whether MASC and PCV-AciCC are two distinct entities or one masquerading as the other.
Design: The surgical pathology archives were searched for low grade salivary gland adenocarcinoma including MASC showing predominantly papillary cystic pattern during a period from 2005 to 2016.. The electronic medical records were reviewed for demographic information. The H&E, IHC and FISH were studied for the presence of ETV6-NTRK3 break apart fusion product.
Results: Of 31 cases of LG adenocarcinoma with papillary cystic pattern, upfront diagnosis of MASC was offered in 18 cases. These were confirmed by IHC and molecular study. Diagnosis of AciCC with papillary cystic pattern was reported in 12 cases and papillary cystadenocarcinoma in one case. These cases were reclassified as MASC after IHC and molecular testing. All the sections showed diffuse strong positivity for mammaglobin, CK7 and S100 with negativity for DOG1 and P63. Luminal positivity for MUC 4 was noted in 93.5% cases; uninterpretable in 6.5% cases due to tissue depletion. 77.4%cases showed ETV6 split signals. FISH was uninterpretable in 22.6 % cases due to more than six years old archival blocks and depletion of the tumor tissue. Parotid was primary site in 77.4% followed by submandibular glands (12.9%) and hard palate(9.6%).
Conclusions: MASC is a distinctive SGT with defining molecular translocation. Our study highlights that papillary cystic variant of AciCCs can masquerade as MASC if classified solely on the architectural growth patterns. IHC and molecular studies are mandatory to rule out MASC. More studies from different geographic areas are necessary to understand tumor biology.

1312 The Landscape of Genomic and Transcriptomic Alterations in Esthesioneuroblastomas

Jisun Kim, Kathleen A Burke, Rodrigo Gularte-Merida, Felipe Geyer, Fresia Pareja, Britta Weigelt, Fernando Schmitt, Brian P Rubin, Ilan Weinreb, Jorge Reis-Filho. Memorial Sloan Kettering Cancer Center, New York, NY; Laboratoire National de Santé / Luxembourg - Anatomie Pathologique, Luxembourg, Luxembourg; Cleveland Clinic, Cleveland, OH; University Health Network, Toronto, Canada.
Background: Esthesioneuroblastoma (ENB) is a rare malignancy originating from olfactory neurosensory cells. The repertoire of genetic alterations in ENBs remains to be elucidated. The aim of this study is to investigate whether ENBs are driven by highly recurrent somatic mutations or fusion genes.
Design: Representative frozen sections of six ENBs and adjacent normal tissue were microdissected. DNA samples were extracted from tumor and normal tissues and successfully subjected to whole-exome sequencing in five cases. RNA samples were extracted from six ENBs and subjected to RNA-sequencing. Somatic singe nucleotide variants were identified with MuTect, small insertions/deletions using Strelka and VarScan 2, and copy number alterations using FACETS. Cancer cell fractions were inferred using ABSOLUTE. Expressed fusion genes were detected using deFUSE and INTEGRATE. Selected mutations and fusion genes were validated by means of Sanger sequencing and reverse transcription PCR, respectively.
Results: 191 non-synonymous somatic mutations were identified across 184 genes among which 73 mutations were validated by RNA-sequencing. Seventeen recurrent and/ or pathogenic somatic mutations were validated by Sanger sequencing (*MACF1, ANKHD1, ARHGEF9, ATM, CNOT10, CSDM1, DCTN1, ITSN1, LMTK2, MAP2K1, MMRN2, MYOCD, RCE1, RORB, SDCCAG8, ZNF471*). The microtubule actin crosslinking factor 1 (*MACF1*) gene was found to be recurrently mutated; both mutations were missense and coupled with loss of heterozygosity of the wild-type allele. RNA-sequencing revealed 223 fusion transcripts, of which an inter-chromosomal in-frame *DHRS2-GSTM2* fusion gene was found to be recurrent in two low-grade ENBs.
Conclusions: ENB is a genetically heterogeneous disease. One recurrent somatic inactivating *MACF1* mutation was identified in two ENBS, and a validated expressed *DHRS2-GSTM2* fusion gene was identified in two low-grade ENBs. Further studies assessing the prevalence of these recurrent alterations in a large cohort of ENBs are warranted.

1313 BRAF V600E Mutations in Infarcted Thyroid Carcinoma

Erik Kouba, Andrew Ford, Charmaine G Brown, Chen Yeh, Hyung-Gyoon Kim, Gene P Siegal, Upender Manne, Isam-Eldin Eltoum. University of Alabama-Birmingham, Birmingham, AL; Circulogene, Inc., Homewood, AL.
Background: Fine needle aspiration (FNA) is a well-established method for the rapid diagnosis of an ultrasound visualized thyroid lesions. A rare occurrence, however, is the near-complete infarction after FNA with subsequent obscuration of histopathological diagnosis. In this study we present one of the largest series of such post-FNA infarctions and our experience with subsequent diagnosis using next generation sequencing for BRAF V600E mutations.
Design: Nine thyroid lesions with extensive to near complete infarctions were identified from our institutional database from 2010 to 2015. From formalin fixed paraffin embedded tissue, tissue was extracted and examined using next generation sequencing for BRAF V600E mutations.
Results: The clinicopathological results are shown in Table 1. The cohort consisted of 2 males and 7 females with a mean (median) age of 53 (55 years). The mean (median) size of lesions was 29 (25 mm). The mean (median) time between FNA and surgery was 35 (38 days). All lesions were infarcted showing complete (~100%), near total (>90%) and extensive (>60%). Overall we found BRAF V600E mutations in infarcted tissue in 44% of cases (4/9).

Case	Gender/ Age (years)	Size (mm)	FNAs prior to surgery (n)	Interval of last FNA to surgery (days)	Surgical Diagnosis*	Extent of infarct	BRAF V600E Mutation present in infarct
1	M/37	12	1	27	FV PTC	Near Total	No
2	F/55	10	1	38	PTC	Near Total	No
3	F/21	25	1	53	TC PTC	Extensive	Yes
4	F/59	55	1	41	PD	Extensive	No
5	F/74	4	1	2	PTC	Near Total	Yes
6	F/88	65	1	37	TC PTC	Extensive	No
7	F/43	1	1	69	PTC	Complete	No
8	F/57	25	2	26	PTC	Extensive	Yes
9	M/46	60	1	14	PTC	Extensive	Yes

*FV PTC, follicular variant, papillary thyroid carcinoma; TC PTC, tall cell variant, papillary thyroid carcinoma; PD, poorly differentiated thyroid carcinoma including insular
Conclusions: Infarction of papillary thyroid lesions after FNA is a rare but well noted occurrence which has not been well characterized to date. Unfortunately, the occurrence can obscure lesional cells making accurate diagnosis difficult. In this study, we characterized one of the largest single institutional series to date of such infarcted tumors. We also showed that next generation sequencing can be useful when performed on infarcted tissue to reveal the nature of infarct and discrepancy between FNA and histology in cases of total infarction.

1314 Tumor Metabolism and ROS Determine Efficacy of HNSCC Therapy by Modulating Immune Status

Rosemarie Krupar, Ravi R Pathak, Christian Idel, Sven Perner, Andrew G Sikora. University Hospital of Luebeck and Research Center Borstel, Luebeck, Germany; Baylor College of Medicine, Houston, TX; University Hospital of Luebeck, Luebeck, Germany.
Background: Tumor immune response and tumor metabolism both affect survival in head and neck squamous cell carcinoma (HNSCC). We assessed interdependencies and prognostic significance of specific immune and metabolic gene signatures within The Cancer Genome Atlas (TCGA) and evaluated underlying signaling mechanisms linking tumor metabolism with immune response in a tumor spheroid/immune cell co-culture model.
Design: Anti-tumor immune response (CD8A) and anaerobic/glycolytic (GLUT1) as well as aerobic (COX5B) tumor metabolism markers were defined according to mRNA up- and down-regulations within the TCGA HNSCC databank. Short-term (20 months) and long-term (60 months) survival were calculated by the Kaplan-Meier method. ROS production of HNSCC cells after glycolysis inhibition by 2-Deoxyglucose (DGL) and *ex vivo* radiation treatment was measured and chemotaxis of human peripheral blood mononuclear cells (PBMC) to HNSCC spheroids was evaluated in the presence or absence of the ROS scavenger N-acetylcysteine (NAC).
Results: The TCGA HNSCC databank analysis included 522 patients. CD8A was more frequently decreased in tumors with high GLUT1 ($p<0.0001$). COX5B had no effect on CD8A. While neither COX5B, nor GLUT1 alone had an impact on outcome, patients with increased CD8A presented with improved long-term survival ($p=0.049$). A patient subgroup with a favorable immuno-metabolic gene signature (high CD8A, high COX5B, low GLUT1) showed improved short-term ($p=0.013$) and long-term ($p=0.048$) survival in comparison to patients with an unfavorable gene signature (low CD8A, low COX5B, high GLUT1). Furthermore, the expression level of the H_2O_2 producing enzyme superoxide dismutase 2 (SOD2) was more frequently up-regulated in tumors with a favorable gene signature ($p=0.047$) implying an involvement of ROS. *In vitro*, ROS production increased, alone and synergistically, with DGL treatment and radiation. In spheroid/immune cell cocultures, DGL treatment combined with radiation led to increased PBMC chemotaxis to HNSCC spheroids. Addition of NAC abrogated this effect indicating a ROS-related signaling mechanism.
Conclusions: Survival following chemoradiotherapy is determined in part by an interplay between tumor metabolism and immune response, potentially via ROS-mediated signaling.

1315 Expression of Cancer Stem Cell Markers in Salivary Gland Basal Cell Adenocarcinoma and Basal Cell Adenoma

Sook-kyung Kwon, Allyn M Lambertz, Robert Robinson. University of Iowa Hospitals and Clinics, Iowa City, IA; The University of Iowa Carver College of Medicine, Iowa City, IA.
Background: Emerging studies have characterized a population of tumorigenic cancer stem cells (CSC) that have the ability to initiate and drive tumor progression in salivary gland malignancies. A sub-population of CSCs have been described in some salivary gland neoplasms but CSC expression in basal cell adenocarcinomas (BCAC) and basal cell adenomas (BCA) has not been sufficiently investigated. These two neoplasms appear cytologically similar but are separated primarily by the presence of invasion in BCAC. In this study, we examined immunohistochemical expression of CSCs in BCAC and for comparison, in the cytologically similar tumor, BCA.
Design: Tissue microarrays of 30 BCAs and 19 BCACs were constructed from paraffin blocks and examined by immunohistochemistry for ALDH, BMI1, CD44, CD133, OCT4, and Podoplanin. Staining on triple replicates of tissue cores were performed and scored, blinded by the diagnosis, based on the intensity of staining (0-3) and percentage

(0-100%), to obtain an H-score (intensity x percentage) of 0-300. The mean H-scores were calculated for BCAs and BCACs and compared using the Student's *t*-test. The Mann-Whitney *U*-test was used to compare the median H-scores for BCAs and BCACs. Statistical tests were 2-tailed with *p*-values <0.05 considered significant.

Results: CSC expression in BCAs and BCACs is summarized in Table 1. The median H-scores for ALDH, CD44, and Podoplanin expression in BCA and BCAC were significantly different (*p* values 0.009, <0.001, and 0.007, respectively), though mean H-scores for these CSC markers were <100 in both tumors. No significant difference in median H-scores for BMI1 and OCT4 was seen in BCA compared to BCAC.

Table 1. CSC expression in BCA vs. BCAC

Antibody	BCA n = 30 Mean H-score	BCAC n = 19 Mean H-score	t-testp-value	U-testp-value
ALDH	55	95	0.009	0.009
BMI1	93	98	0.78	0.968
CD44	58	83	0.13	<0.001
OCT4	0	0	no value	1
Podoplanin	0	19	<0.001	0.007

Conclusions: The expression of ALDH, CD44, and Podoplanin is significantly greater in BCAC compared to BCA, however the mean H-scores for these three markers were <100 in both tumors. From this study it appears that both BCAC and BCA have relatively low levels of expression of CSC markers yet BCAC shows significantly higher expression, suggesting a true difference between these neoplasms at the molecular level which may relate to differing histologic and biologic behavior.

1316 Computer Extracted Features of Nuclear Architecture in H&E Sectionsare Predictive of Disease Specific Survival Inoral Cavity Squamous Cell Carcinoma Patients

Cheng Lu, James Lewis, Anant Madabhushi. Case Western Reserve University, Cleveland, OH; Vanderbilt University Medical Center, Nashville, TN.

Background: Oral cavity squamous cell carcinoma (OCSCC) is one of the most common head and neck carcinomas, and its morbidity and mortality are increasing worldwide. Prognosis remains poor despite advances in treatment. Histologic features associate with prognosis, but only modestly, when assessed visually by pathologists. In this study, we present preliminary findings that patients with aggressive tumors can be distinguished from those with more indolent ones using nuclear architecture features assessed by computerized analysis of digitized H&E stained sections.

Design: A tissue microarray of 115 primary OCSCC was digitally scanned and 50 cases selected at random for modeling with the other 65 for validation. Nuclei were segmented using a watershed method and local/global graphs were constructed based on the centroids of segmented nuclei. Based on the nuclei graph, nuclear architectural features were extracted and analyzed, and the features most discriminative of patient death from disease were utilized to train a classifier. The five best quantitative histomorphometric features were identified using Wilcoxon rank sum test within the training cohort. A quadratic discriminant classifier (Oral Cavity Histomorphometric-Based Image Classifier or OHbIC), was created and validated in the independent cohort of 65 patients.

Results: The five best quantitative histomorphometric features are all from a feature set which captures statistics of co-occurrence nuclei with similar morphology. In univariate survival analysis, OHbIC positive patients had significantly poorer disease-specific survival (p=0.0268). In multivariate analysis, controlling for the major prognostic variables such as T and N-classification and resection margin status, positive OHbIC results were independently predictive of poorer disease-specific survival [hazard ratio with 95% CI = 11.023 (2.62-46.38); p=0.001].

Conclusions: Computerized histomorphometrically-derived features of nuclear architecture derived from digitally-scanned tumor H&E slides are strongly and independently predictive of patient survival in OCSCC. This may form the basis for a future predictive image analysis classifier that can be used in tailoring treatments for OCSCC patients.

1317 HPV Genotyping in Head and Neck Papillomas(HNP): An Institutional Experience

Abul Ala Syed Rifat Mannan, Dana Gao, Aneta Waluszko, Wenjing Shi, David Y Zhang, Fei Ye. Mt Sinai Hospital, New York, NY.

Background: HPV infection is a major risk factor for development of benign and malignant mucosal head and neck lesions. There is limited data on association of HPV with benign HNPs. Here we report frequency of HPV subtypes in HNPs diagnosed at our institution.

Design: Clinical and pathologic features were reviewed for HNPs diagnosed between 2012 and 2015.Maxwell 16 FFPE Tissue LEV DNA Kit was used for DNA tissue extraction, and Real-time PCR testing with pan-HPV primers (GP5+ and GP6+) and primers/probes specific for HPV16 and HPV18, followed by Sanger sequencing of samples positive for HPV but negative for HPV16/18, was used for HPV genotyping.

Results: 100 cases of HNPs were genotyped(73 males,23 females,average age 47.4 yrs, range 6-78 yrs). Of these 93 were benign HNPs and 7 were inverted papillomas. Locations included oral cavity (n= 23), tongue (n= 8), tonsil (n= 9), oropharynx (n=6), larynx (n= 35), sinonasal tract (n= 19, including 7 inverted papillomas).HPV DNA was positive in 37 cases (37%).HPV 6 was most prevalent (n=19;51.4%), followed by HPV11(n=10; 27%),HPV16 (n=5; 13.5%),and HPV32 (n=1; 2.7%).HPV subtype was indeterminate in 2 cases (5.4%).Tongue (62.5%) and larynx (57.1%) showed highest HPV positivity. Of the 5 HPV 16 + cases, 2 had associated squamous cell carcinoma (SCC) of the tonsil, 1 had SCC of skin (neck); 2 had no known associated cancers. Of HPV positive cases, 75.7% (28/37)were male and 24.3% (9/37)female**.** p16 IHC was done in 10 cases (negative 1, weak 6 and diffuse strong 3). Diffuse positivity was seen in those with HPV 16.

Site (n)	GenderM:F	HPV6 (n)	HPV11 (n)	HPV16 (n)	Others (n)	HPV (-)(n)	HPV +(%)
Oral cavity(23)	18:5	0	1	0	1 indeter-minate	21	8.7
Tongue(8)	4:4	1	1	2	1 HPV32	3	62.5
Tonsil(9)	6:3	0	0	2	0	7	22.2
Oropharynx(6)	4:2	0	1	0	0	5	14.3
Sinonasal(19)	17:2	3	4	0	0	12	36.8
Larynx(35)	24:11	15	3	1	1 indeter-minate	15	57.1
Total(100)	73:27	19	10	5	3	63	37

Conclusions: Our data and published study (Andratschke et al., HNO. 2015;63:768) reveal prevalence of HPV in HNPs is about 37%, which confirms an important role of HPV in development of benign HNPs. Diagnosis of HNPs on histology alone should be made with caution and reflex HPV genotyping is recommended. In cases of low risk HPV (6 and 11) associated HNPs, a conservative management may suffice. However, those with high-risk HPV subtypes warrant close surveillance to identify possible underlying SCC.

1318 The Value of Hyams Grade in an Endoscopically Treated Cohort of Olfactory Neuroblastoma

Stacey K Mardekian, Carl H Snyderman, Aron Z Pollack, Paul Gardner, Raja R Seethala. University of Pittsburgh Medical Center, PA.

Background: Hyams grading is considered a prognosticator in olfactory neuroblastoma (ONB), but grading criteria are subjective, and predate ancillary testing and modern surgical approaches. We propose detailed grading criteria definitions and apply them to a unique cohort treated mainly by endonasal endoscopic approach (EEA).

Design: 50 of 69 ONB seen in a 22 year period at our institution had primary tumor available for review. The majority (75%) were treated surgically by EEA and received adjuvant radiotherapy (90%). Mean follow-up was 59.2 months. A traditional Hyams grade had been assigned in 68% (34/50) cases. A modified version of the Hyams grading was developed (Table 1) and utilized to assign each tumor a score of I-IV. Clinicopathologic parameters were correlated with outcomes using univariate Cox regression analysis.

Table 1.

	I	II	III	IV
Architecture	>75% large lobules (fit in 10x field)	>25% small lobules (fit in 20-40x field)		>5% frank infiltration (diffuse sheets, cords, single cells)
Neurofibrillary matrix	>25% of surface area	<25% of surface area		None
Nuclear pleomorphism	<2:1 size variation		>50% of tumor with 2-<4:1 size variation	>10% of tumor with ≥4:1 size variation
Rosettes	Pineocytomatous	Homer Wright	Flexner-Wintersteiner	None
Mitotic count per 10 HPF	0	1-2	3-9	10+
Necrosis	None		Punctate	Confluent

Results: The mean age at presentation was 51.1 years (range: 15.5-83.7 years) with a male predilection 1.6:1. Recurrence rate was 26%. The prevalence of lymph node and distant metastases were 18% and 10% respectively. Original Hyams grade distribution was: I: 6%, II: 65%, III: 26%, and IV: 3%. Modified Hyams grade distribution on all cases was: grade II: 54%, grade III: 42%, and grade IV: 4% with no grade I cases.

Only lymph node (HR: 10.658, p=0.041) and distant metastases (HR: 16.951, p=0.015) correlated with disease specific survival (DSS). Only age at diagnosis correlated with disease free survival (DFS) (HR: 1.060, p=0.038). Original Hyams grade did not correlate with DFS (HR: 0.731, p=0.645) or DSS (HR: 0.626, p=0.532). Modified Hyams grade did not correlate with DSS (HR: 1.229, p=0.721), but trended towards correlation with DFS (HR: 1.829, p=0.162).

Conclusions: Hyams grade may not be as relevant in a modern ONB cohort. However, modified Hyams grade offers a slight improvement over original Hyams grade. Hyams grade I and IV are rare and likely unnecessary, suggesting reduction of ONB grading to simply high and low.

1319 Usefulness of NKX2.2 Immunohistochemistry in the Sinonasal Small Round Blue Cell Tumor Differential Diagnosis

Austin McCuiston, Justin A Bishop. Johns Hopkins University School of Medicine, Baltimore, MD.

Background: NKX2.2 is a new marker for Ewing sarcoma/PNET that has been reported to be sensitive and specific. It has not, however, been investigated specifically in the sinonasal small round blue cell tumor (SRBCT) differential diagnosis which includes many tumors specific to that site, including olfactory neuroblastoma, SNUC, and teratocarcinosarcoma. It has also not been investigated in the newly-described adamantinoma-like variant of Ewing sarcoma.

Design: Immunohistochemistry for NKX2.2 was performed on 169 poorly differentiated sinonasal neoplasms: 73 squamous cell carcinomas (67 poorly differentiated, non-keratinizing, or basaloid types and 6 nasopharyngeal carcinomas), 46 olfactory

neuroblastomas, 8 sinonasal undifferentiated carcinomas (SNUCs), 6 melanomas, 7 Ewing sarcomas, 6 SMARCB1-deficient carcinomas, 5 teratocarcinosarcomas, 5 alveolar rhabdomyosarcomas, 4 solid adenoid cystic carcinomas, 4 NK/T cell lymphomas, 3 NUT midline carcinomas, and 2 small cell carcinomas.

Results: NKX2.2 was positive in 7 of 7 (100%) Ewing sarcomas, including 4 adamantinoma-like variant (all diffuse, 4 strong and 2 weak). It was also positive in 4 of 5 (80%) teratocarcinosarcomas (always strong but focal), 12 of 46 (26%) olfactory neuroblastomas (all diffuse, 2 strong and 10 weak), 4 of 6 melanomas (2 diffuse, 2 focal, all weak), and 1 of 2 small cell carcinomas (diffuse and strong). All squamous cell carcinomas, NUT midline carcinomas, SMARCB1-deficient carcinomas, SNUCs, solid adenoid cystic carcinomas, NK/T cell lymphomas, and alveolar rhabdomyosarcomas were negative.

Conclusions: In the sinonasal SRBCT differential diagnosis, NKX2.2 is a useful and very sensitive marker for Ewing sarcoma/PNET including the adamantinoma-like variant. At the same time, it is not entirely specific, as it will be positive in a subset of other neuroendocrine/neuroectodermal tumors. As a result, NKX2.2 must be utilized as part of an immunohistochemical panel with other markers, especially cytokeratins, melanoma markers (such as S100, Melan-A and SOX10), and CD99.

1320 Novel Mutations in Sinonasal Squamous Cell Carcinoma Detected Using Next Generation Sequencing

Gordon AG McKenzie, Taneisha McFarlane, Sandra Hing, Geraldine Thomas, Ann Sandison. Imperial College London, London, United Kingdom; Hull and East Yorkshire Hospitals NHS Trust, Hull, East Yorkshire, United Kingdom.

Background: Sinonasal squamous cell carcinomas (SNSCCs) comprise 80% of sinonasal malignancies. The histopathological distinction between entities, including inverted sinonasal papilloma (ISP) and low-grade SNSCC lacks clarity, adding complexity to surgical management decisions. In this pilot study, we employed next-generation sequencing (NGS) in effort to identify novel molecular aberrations within the ISP-SNSCC spectrum, which could serve as biomarkers or potential therapeutic targets.

Design: DNA was extracted from archived formalin-fixed paraffin-embedded specimens from 10 patients creating a cohort of ISPs with and without atypia, sinonasal mucosal dysplasia, low-grade SNSCC, well- and poorly-differentiated SNSCC. Targeted NGS was performed using the Life Technologies' Ion AmpliSeq™ Cancer Hotspot Panel v2 as a sequencing library. Raw sequencing data was captured using Ion variant caller and comparatively analyzed, with reference to the Catalogue of Somatic Mutations in Cancer (COSMIC) database.

Results: There were 121 variants detected (range 2-73 per sample) where 18 (15%) were intronic and excluded. Twenty (17%) COSMIC mutations from 14 genes were identified and none had specifically been reported in SNSCC. Six genes with COSMIC mutations were known to be associated with SNSCC (*TP53*, *RB1*, *AKT1*, *PIK3CA*, *MET* and *CDKN2A*). To the best of our knowledge, we detected eight previously unassociated genes with COSMIC mutations (*ATM*, *IDH1*, *PTPN11*, *RET*, *VHL*, *FBXWL*, *APC* and *FLT3*). A COSMIC missense mutation in *ATM* (c.1009C>T) was present in both an ISP and unpaired low-grade SNSCC. An apparent missense single nucleotide variant was identified in *SMARCB1* (c.215C>A), which was detected in an ISP, two ISPs with atypia and residual atypia following resection of a low-grade SNSCC. An insertion in *EGFR* (c.2308_2309insACAACCCCC) was found in an ISP (and its associated dysplasia), a low-grade SNSCC and a frank SNSCC.

Conclusions: NGS can be employed to detect novel mutations in the ISP-SNSCC spectrum, which has hitherto been understudied. We demonstrate previously unreported COSMIC mutations in eight genes. The potential of the *SMARCB1* variant detected to serve as a biomarker of atypia is interesting, as *SMARCB1* loss of function has been noted in sinonasal carcinomas with rhabdoid cytomorphology. The finding of a specific cancer-associated insertion in *EGFR* across the ISP-SNSCC spectrum further supports its potential as a biomarker of impending malignancy.

1321 HMGA2 Is a Specific Immunohistochemical Marker for Pleomorphic Adenoma and Carcinoma Ex-Pleomorphic Adenoma

Jeffrey Mito, Vickie Y Jo, Paola Dal Cin, Jeffrey F Krane. Brigham and Women's Hospital, Boston, MA.

Background: The accurate classification of salivary gland neoplasms is often challenging due to the morphologic heterogeneity of these tumors. Previous studies have identified recurrent translocations involving High Mobility Group A2 (*HMGA2)* in a subset of pleomorphic adenomas (PA) and carcinoma ex-pleomorphic adenomas (CA ex-PA). We evaluated the frequency of HMGA2 expression in PA and CA ex-PA and determined the potential diagnostic utility of HMGA2 immunohistochemistry in a broad panel of salivary gland tumors.

Design: 190 salivary gland tumors including: PA (50), CA ex-PA (25), adenoid cystic carcinoma (27), basal cell adenoma (BCA) (19), salivary duct carcinoma (13), polymorphous low grade adenocarcinoma (12), mucoepidermoid carcinoma (12), acinic cell carcinoma (11), epithelial-myoepithelial carcinoma (9), mammary analogue secretory carcinoma (6), myoepithelioma (3), basal cell adenocarcinoma (1), sarcoma ex-PA (1), and oncocytoma (1) were identified and immunohistochemical staining for HMGA2 was performed. The presence and extent of nuclear staining was evaluated. FISH for *HMGA2* rearrangement was performed on a subset of tumors.

Results: Nuclear HMGA2 expression was identified in 14 PAs (28.0%) and 6 CA ex-PAs (24.0%). HMGA2 expression was strong and diffuse throughout all PAs and half of the cases of CA ex-PA. In the remaining 3 cases of CA ex-PA, HMGA2 showed limited weak-to-moderate multifocal staining within the carcinomatous component, while strong and diffuse HMGA2 expression was retained in residual PA. One case each of myoepithelioma and BCA showed strong and diffuse expression of HMGA2. Review of both cases suggested they may represent misclassified PAs as ductal structures were identified in the case of myoepithelioma and the BCA lacked evidence of an activating β-catenin mutation. Both cases were reclassified as PA. Among the remaining salivary gland tumors: 3 *de novo* salivary duct carcinomas (23.1%) and 3 epithelial-myoepithelial carcinomas (33.3%) showed limited HMGA2 expression. FISH for *HMGA2* rearrangement was successfully performed on a subset of tumors and showed that diffuse HMGA2 expression in PA and CA ex-PA was associated with rearrangement of the *HMGA2* locus in 2 of 2 tested PA/CA-ex PA cases, while 2 cases of *de novo* salivary duct carcinoma with limited HMGA2 expression and 1 case of CA ex-PA without HMGA2 expression showed no rearrangement of the HMGA2 locus.

Conclusions: Strong and diffuse HMGA2 protein expression is a specific (99.1%) marker for PA and CA ex-PA that correlates with rearrangement of the *HMGA2* locus.

1322 LEF1 Is S Sensitive Marker of Cribriform Morular Variant of Papillary Thyroid Carcinoma

Shalini Mohindra, Hany Sakr, Charles D Sturgis, Christine N Booth, Deborah Chute. Cleveland Clinic, Cleveland, OH.

Background: Cribriform morular variant of PTC (CMVPTC) activates the CTNNB1/Wnt pathway with nuclear accumulation of B-catenin and LEF1. The utility of LEF1 in the diagnosis of CMVPTC has not been previously studied.

Design: IHC for LEF1 was performed on 7 CMVPTC, 15 normal, 6 CLT, 5 Graves,25 NH, 30 PTCs, 25 FC, 25 HCC and 21 UTC. LEF1 immunostain was scored based on the intensity of the stain (0= no nuclear stain, 1= weak nuclear stain, less than a lymphocyte and 2= strong nuclear stain, as intense as a lymphocyte) and percentage of cells positive at each intensity, for a maximum total score of 200.

Results: Please see tables 1 for results of LEF1 IHC staining. The sensitivity(SS) and specificity(SP) of LEF1 to differentiate PTC and CMVPTC is presented in table 2. The best clinical threshold is ≥30% at 2+ with a SS and SP of 85.7% and 98%, respectively. One CMVPTC was negative for LEF1 and nuclear beta-catenin. If excluded, the SS and SP both increased to 100%.

LEF1 staining by total score and mean % intensity

	Total Score				Mean % Intensity		
Diagnosis	<50	51-100	101-150	>150	0	1+	2+
Benign							
Normal Thyroid	15	0	0	0	81	18	0
Nodular hyperplasia (NH)	23	2	0	0	87	13	0
Lymphocytic thyroiditis (CLT)	5	1	0	0	70	27	3
Graves Ds	5	0	0	0	68	30	2
Malignant							
PTC	25	5	0	0	81	19	0
CMVPTC	1	0	2	4	15	21	65
Follicular ca (FC)	21	3	1	0	81	18	1
Hurthle cell ca (HCC)	21	4	0	0	83	17	0
Anaplastic (UTC)	11	8	2	0	61	27	12

Sensitivity and Specificity of LEF1 for CMVPTC using various thresholds

LEF1 Total score	Sensitivity	Specificity
≥ 100	86	97
≥ 150	57	99
LEF1 2+%		
≥ 10%	86	91
≥ 30%	86	98
≥ 50%	57	100

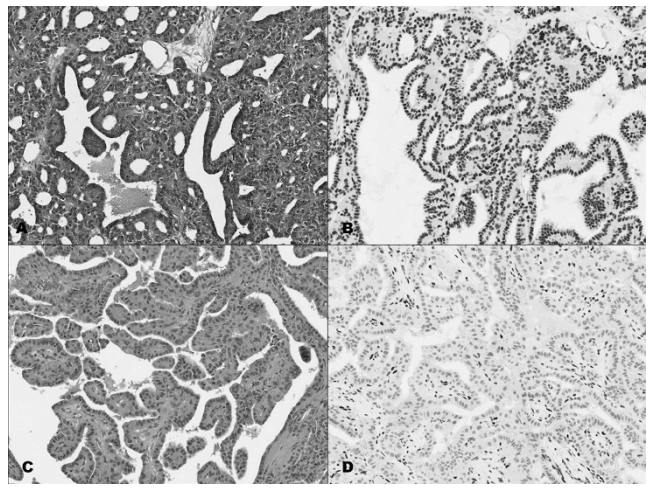

A CMVPTC 20x; B CMVPTC LEF1 20x; C Classical PTC 20x; D Classical PTC LEF1

Conclusions: LEF1 immunostain is highly sensitive and specific for CMVPTC, especially in the setting of a PTC neoplasm. The pattern of staining is important with ≥ 30% of cells showing strong nuclear staining.

1323 Traditional Grading of Oropharyngeal and Non-Oropharyngeal Squamous Cell Carcinomas in the HPV Era

Kathleen Montgomery, Mitra Mehrad, Krystle Lang Kuhs, James Lewis. Vanderbilt University Medical Center, Nashville, TN.

Background: In recent years, HPV-positive oropharyngeal squamous cell carcinoma (HPV+OPSCC) has become recognized as a distinct clinical entity, differing from HPV-negative OPSCC in molecular pathophysiology, epidemiology, and prognosis. The histologic grade, or differentiation, of head and neck SCC (HNSCC), including OPSCC, has been found to correlate with survival, albeit modestly, and CAP and RCPath recommend reporting a grade for all HNSCC. Few studies, though, have investigated traditional grading of OPSCC in the HPV era. Since most HPV+OPSCC appear poorly differentiated by classical grading while having a better prognosis than HPV- SCC, traditional grading may not be of value.

Design: Digitally-scanned tissue microarrays (2 mm and 0.6 mm punches) of H&E stained slides from 291 retrospectively identified HNSCC patients were examined: 151 HPV+OPSCC (p16 and mRNA *in situ* hybridization [ISH] dual positive), 42 HPV-OPSCC (p16/mRNA ISH dual negative) and 60 non-OPSCC. One study head and neck pathologist provided each a histologic grade (well-, moderately-, or poorly-differentiated) and also assessed keratinization, tumor-stroma ratios, and nest size (1, 2, or 3). The association between histologic features and overall (OS) and disease-specific survival (DSS) were evaluated in Cox proportional hazard models.

Results: Of the 291 cancers graded, 15 were well- (WD), 138 moderately- (MD), and 138 poorly-differentiated (PD). In univariate analysis, PD cases had increased overall ($p=0.01$) and disease-specific ($p=0.02$) survival, but these associations were not present after controlling for HPV status. No association between tumor grade and survival was found in subgroup analyses performed after stratification by HPV status and tumor site. Similar findings were observed with degree of keratinization, and neither tumor:stroma ratio nor nest size correlated with survival.

Conclusions: In our cohort, PD and keratin-absent tumors had increased overall and disease-specific survival over WD/MD ones. However, HPV+OPSCC tends to be poorly differentiated and lack keratin, yet have a favorable prognosis. The fact that grade was not prognostic after controlling for HPV status or in subgroup analysis suggest that, although it is widely recommended to provide grade in routine pathology reporting, it may not be useful in either HPV+OPSCC or in HNSCC more broadly.

1324 Sinonasal Small Cell Neuroendocrine Carcinoma (SNEC): Clinicopathological Study of 37 Cases

Ashvini Natu, Asawari Patil, Munita Bal, Rajiv Kumar, Shubhada Kane. Tata Memorial Centre, Mumbai, Maharashtra, India.

Background: SNEC is a rare but aggressive tumor of sinonasal tract. Though it shows histomorphology similar to its pulmonary counterpart, it is a close differential diagnosis for olfactory neuroblastoma (ONB) along with other poorly differentiated carcinoma like sinonasal undifferentiated carcinoma (SNUC) and poorly differentiated squamous cell carcinoma. In this study we describe the clinicopathological profile of 37 cases of SNEC diagnosed at a tertiary cancer center.

Design: All cases of SNEC diagnosed in our institute from January 2011 to August 2015 were retrieved from pathology archives. The hematoxylin-eosin(H-E) slides as well as immunohistochemistry(IHC) slides were reviewed. Histopathological parameters reviewed include: architectural pattern, cytomorphological features (including cell type, cytoplasm, nuclei and nucleoli), presence of necrosis, atypical mitosis and apoptosis. Clinical details and radiological findings were obtained from electronic medical records.

Results: Thirty seven cases of SNEC were identified, with a male to female ratio of 3.6:1 and an age range of 19-68 years(mean=44.3 years). The duration of symptoms was known in 32 cases, ranging from 15 days to 2 years(mean=4.8 months). The commonest site was nasal cavity(16 cases) followed by maxilla(10 cases), ethmoid(5 cases), frontal(1 case) and sphenoid(1 case). Four cases showed tumor involving multiple sites. Radiological findings were known for 34 cases, of which 16 cases showed intracranial extension while 17 cases showed intraorbital extension. The commonest architectural pattern was tumor cells in sheets, nests and clusters. Cells were usually small to medium sized, round to oval shaped with scanty cytoplasm. Majority of the cases showed hyperchromatic nuclei with indistinct nucleoli. Increase in mitoses with atypical mitoses and apoptosis was seen in most of the cases. Necrosis was common (seen in 28 cases). Nine cases showed desmoplastic reaction in stroma. Two cases showed an unusual morphological feature - pagetoid spread of tumor cells in the overlying mucosa, which was confirmed by IHC. This feature has not been described in literature. Features seen in ONB such as rosette formation and neurofibrillary matrix, were not seen in any of these cases. IHC studies were available in all 37 cases. The commonest markers expressed were Pancytokeratins (AE1/AE3, CK) and one or more neuroendocrine markers (Synaptophysin, Chromogranin, CD56, NSE).

Conclusions: SNEC needs to be differentiated from other small round blue cell malignant tumors of sinonasal tract as it is associated with poor outcome and needs multimodal treatment.

1325 Warthin's Tumor of the Parotid Gland: A Simple Lesion with Complex Clinical Implications; a Clinical Pathologic Review

Anam Naumaan, Ritu Ghai, Paolo Gattuso. Rush University Medical Center, Chicago, IL.

Background: Warthin's tumor (WT) is the second most common benign tumor of the salivary glands, majority involving the parotid gland. Characteristic clinical features include, painless, slow growing lesion which can be multifocal and bilateral. However, the clinical significance of a diagnosis of WT is not well understood or studied. We investigated the relationship between WT and synchronous or metachronous salivary and extra-salivary gland lesions associated with this neoplasm and their clinical significance.

Design: Between 1993 to September 2016, the pathology files at our institution were reviewed for a diagnosis of WT. The clinical and pathologic data was reviewed in detail for other lesions occurring in patients with diagnosis of WT, either at the same time/within the same year (synchronous), or at another time (metachronous).

Results: A total of 63 cases of WT were identified (42 males, 21 females), with the age ranging from 32 to 78 years. 22 cases (35%) with additional lesions were identified. Of these 22, 15(68.2%) were synchronous, 5(22.7%) metachronous, and 2(9.1%) were both synchronous and metachronous lesions. In cases with metachronous lesions, the second lesion was diagnosed within 5 years of diagnosis of the first lesion, with only 1 case where the second lesion was diagnosed at 9 years. There were 3(13.6%) cases with 3 lesions each. Of 22 cases, 11(50%) had head and neck tumors, 6(27.3%) had lung tumors, 3(13.6%) had hematologic malignancies, while there was one case each of myxoinflammatory sarcoma, breast cancer with renal cancer, and sarcoidosis. Of the 11 head and neck tumors, 7(63.6%) were malignant (5 squamous cell carcinoma, 2 ductal type adenocarcinoma) and 4(36.4%) benign (2 pleomorphic adenoma, 2 lymphoepithelial cysts); (8 synchronous, 3 metachronous). Of the 6 lung tumors (5 synchronous, 1 metachronous) there were 4(66.7%) cases of adenocarcinoma and 2(33.3%) of small cell carcinoma. The hematologic malignancies included 2 metachronous (1 case of CLL and Hodgkin's lymphoma, respectively) and 1 synchronous B-call lymphoma. It was also noted that in 6 out of 7 metachronous lesions, WT was not the first lesion.

Conclusions: Analysis of our data shows that there is an association of WT with other tumors, either synchronous or metachronous. The most common association is with head and neck tumors, and lung carcinomas. It might be helpful to screen or follow up patients with WT for other head and neck tumors, as well as lung carcinoma following a diagnosis of WT.

1326 NIFTP - Cases for Reclassification – A 10 Year Review and Workload Assessment

Kevin O'Hare, Esther O'Regan, Aftab Khattak, Marie Louise Healy, Mary Toner. Saint James Hospital, Dublin, Ireland.

Background: In March 2016, after conducting an international retrospective study on encapsulated follicular variant of papillary thyroid carcinoma (EFVPTC), a panel of experts made the case for reclassifying some EFVPTC as non-invasive follicular thyroid neoplasm with papillary-like nuclear features (NIFTP), changing the nomenclature from a malignant to a non-malignant entity Following publication of the JAMA paper, many requests to review cases for re classification were received from clinicians which prompted this review of cases. We also assessed the workload involved in the slide review.

Design: A 10 year (2007-2016) search of all papillary thyroid carcinoma (PTC) thyroid resection histology reports was performed. Cases were selected as potential NIFTP candidates based on report review alone. Following this initial triage, the slides of the remaining cases were reviewed independently by two consultant histopathologists and the number of slides required to complete the review was recorded. Once a single exclusion criterion was met, no further slides were reviewed.

Results: Of the 545 reports reviewed, 71 cases were identified as potential NIFTP cases.49 cases were external cases and histology was not available.

Of the remaining 22 cases, 5 (22.7%) met the criteria for reclassification as NIFTP. 17 cases were excluded based on the histologic criteria as listed in table 1.

Exclusion Criteria	Number of cases excluded
Capsular invasion	6
Papillary growth>1%	5
Solid trabecular growth pattern >30%	4
Psammoma bodies	1
Capsule not adequately sampled	1

The 17 non NIFTP cases required review of 114 slides, range 2-28, mean 6.7, median 5.5 slides per case; 5 NIFTP cases where all slides were reviewed required review of 58 slides range 7-20, mean 11.6, median 12 slides per case

Conclusions: NIFTP accounted for 0.9% of all PTCS over this 10 year period. Review of just the reports was sufficient to exclude NIFTP in the majority of cases, and in those that required slide review, exclusion criteria were identified after review of an average of 5.7 slides per case. The issue of availability of external material is a limitation in a tertiary referral centre.

1327 Up-Regulation of PLAG1 and HMGA2 mRNA in Salivary Gland Neoplasms

Viren Patel, Chao Wu, Xunda Luo, Nirag Jhala, Jasvir S Khurana, Jian Huang, He Wang. Temple University Hospital, Philadelphia, PA; Fox Chase Cancer Center, Philadelphia, PA.

Background: Salivary Gland neoplasms has varied histology and diagnostically challenging on small biopsies and on fine needle aspiration, especially between Pleomorphic adenoma (PA) and other basaloid neoplasms like Basal cell adenoma (BCA), Polymorphous Low-grade adenocarcinoma (PLGA) and Adenoid cystic carcinoma (AdCC). Ancillary studies to date have been determined to be of limited value. It's suggested that two genes may be differentially expressed in pleomorphic adenomas (pleomorphic adenoma gene 1, or PLAG1, and high mobility group AT-hook 2, or HMGA2). We hypothesized that quantitation of PLAG1 and HMGA2 mRNA levels could serve as important tool for differentiating challenging PAs from other basal cell neoplasms.

Design: In the present study, we extracted RNA samples from (104) formalin-fixed, paraffin-embedded tissue blocks [62 PAs, 3 Pleomorphic Ex carcinoma (EXPA), 5 Myoepithelial carcinoma (ME), 5 Mucoepidermoid carcinoma (MU), 4 PLGA, 8

Warthins tumor, 4 AdCC, 5 Salivary duct adenocarcinoma (AdCA), 2 BCA, 6 normal salivary gland controls]. Specific primers for PLAG1 and HMG2 were designed and tested in tumor cell lines. mRNA levels of the genes were measured by quantitative reverse transcription polymerase chain reaction, and compared between salivary gland neoplasms and control groups.

Results: PLGA1 and HMGA2 levels in the control group were 0.80 ± 0.34 (mean ± SD) and 0.04 ± 0.07, respectively. An empirical cutoff of four times of the control PLGA1/HMGA2 means (4 x mean) was implemented to categorize cases with known histological diagnoses as positive (at least one measure was greater than 4 x mean) or negative (both PLGA1 and HMGA2 levels were lower than 4 x mean) for over-expression. The 4 x mean cutoff identified 56.5% of PA, 66.7% of EXPA, 40% of ME, 20% of AdCA, 20% of MU, and 12.5% of WA cases as positive for over-expression of at least one gene, and identified all AdCC, BCA, and PLGA cases as negative for over-expression. The difference in detected cases with over-expression (i.e. sensitivity) among disease groups was statistically significant (Fisher exact test value = 16.623, p = 0.012).

Conclusions: Either PLAG1 and HMGA2 gene overexpression levels could be very useful diagnostic tools for challenging PAs to differentiate from basloid lesions but one should warranted cautions as it can be positive in myoepithelial carcinoma, salivary duct adenocarcinoma, mucoepidermoid carcinoma and in rare cases of warthins tumor.

1328 Epidemiology of Patients Diagnosed with Oral Cavity Squamous Cell Carcinoma in South Florida

Yolanda Payne-jameau, Paula S Espinal, Darcy A Kerr, Stuart J Herna, Tanner D Corse, Ronda Sanders, Carmen Gomez-Fernandez. University of Miami Miller School of Medicine, Jackson Memorial Hospital and Sylvester Comprehensive Cancer Center, Miami, FL.

Background: Squamous cell carcinoma (SCC) is the most common malignancy in the oral cavity, representing 80-90% of all malignant neoplasms. While the Surveillance, Epidemiology, and End Results (SEER) program collects data on cancer cases from various locations and sources throughout the United States, it does not include Florida. The Hispanic/Latino community is the largest minority group in the United States, now representing approximately 17% of the population and growing, and it comprises 70% of the total population in Miami, Florida. This study aims to assess the epidemiology of patients diagnosed with oral cavity SCC in a Miami, Florida based cohort.

Design: This is a retrospective cohort study of 4701 patients from 3 South Florida health centers, Jackson Memorial Hospital (tertiary care), University of Miami Hospital and Sylvester Comprehensive Cancer Center, diagnosed with oral cavity SCC over a 10-year period (2005-2015). We categorized our cohort as Non-Hispanic White (NHW), Non-Hispanic Black (NHB), and the Hispanic group as Caribbean Latino (CL) and Non-Caribbean (NCL) Latino, due to the strong African heritage of Caribbean countries.

Results: Overall, our sample consisted of NHW (56%), NHB (7.3%), CL (18%), NCL (16%), and other racial/ethnic groups (2.7%). Oral cavity SCC was more common in men than women (OR 3.58, p=0.003) with men representing 73.11%. Mean patient age was 73 years-old and affected women were a decade older than men (p<0.001). Site distribution showed that the border of the tongue (37%), alveolar mucosa/gingiva (20%) and floor of mouth/ventral tongue (19%) were the most commonly affected sites, with no differences for males and females (p=0.091). Smoking and alcohol intake were more common in NHW than other race/ethnicity groups (OR 3.58, p=0.003 and 4.33, p= 0.001, respectively). CL were more associated with smoking status (OR 1.81, p=0.007) and weekly alcohol intake (OR 3.20, p=0.001), compare to NCL. NHB were less associated with smoking (OR 3.20, p=0.015) than CL.

Conclusions: These results reflect epidemiological characteristics of oral cavity SCC and can serve as a useful guide to researchers contemplating community-based research in populations with significant disparities, such as South Florida. While the Hispanic/Latino community comprises 70% of the population in this region, only 34% of oral cavity SCC affected this population; further exploration of factors including socioeconomic factors underlying this apparent discrepancy is warranted.

1329 Correlation of PDL-1 with STAT-Protein Expression in p16-Positive and -Negative Head and Neck Squamous Cell Carcinomas

Kate Poropatich, Germaine Gaber, Ajit Paintal, Kalliopi P Siziopikou, Sandeep Samant, Bharat Mittal. Northwestern University, Chicago, IL.

Background: While IFN-y is understood to be an extrinsic stimulator of PDL-1 expression on tumor cells, intratumoral regulators of PD-L1 expression are not well characterized. Like IFN-y, STAT3, which is overexpressed in head and neck squamous cell carcinomas (HNSCC), utilizes JAK2 cell signaling. In this study we investigate whether there is a predictive expression pattern among PD-L1, STAT-3 and STAT-1 in p16-positive and -negative HNSCC.

Design: We analyzed 73 cases of oropharyngeal carcinoma (p16-positive= 56, p16-negative= 17). IHC was performed using PD-L1 (E1L3N), STAT-3 (F-2) and STAT-1 (C-136) antibodies. Reactivity was graded as 0-3 based on the percentage of protein expression. PD-L1 reactivity was recorded as the percent of staining on both tumor (T) and peri-tumoral lymphocytes (L): Score 0 = <1%, 1= 1-5%, 2= 6-15%, 3= >15%.

Results: PD-L1 and STAT-1 had a statistically significant positive correlation (r^2= 11.17%, p= 0.0065).

Figure 1: Correlation of PD-L1 with STAT-1 expression on tumor cells in HNSCC

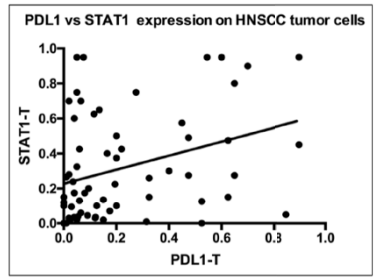

PD-L1 and STAT-3 had a weakly positive correlation that was not significant. Compared to p16-negative cases, significantly more p16-positive cases had a score of 3 for PDL-1 tumor expression (p= 0.032) and STAT-3 tumor expression (p= 0.029).

Figure 2: Expression of PD-L1, STAT-1 and STAT-3 on p16+ and p16- cases

	PD-L1(T)*	PD-L1(L)*	STAT-1*	STAT-3 (T)*
Grade	p16-pos			
	p16-neg			
0	9.09 (4)	2.13 (1)	4.17 (2)	0 (0)
	14.29 (2)	16.67 (2)	7.14 (1)	7.14 (1)
1	25.0 (11)	6.38 (3)	29.17 (14)	1.96 (1)
	21.43 (3)	8.33 (1)	4.29 (1)	7.14 (1)
2	13.64 (6)	42.55 (20)	50.0 (24)	25.49 (13)
	35.71 (5)	25.0 (3)	35.71 (5)	35.71 (5)
3	52.27 (23)	48.94 (23)	16.67 (8)	72.55 (37)
	28.57 (4)	50.0 (6)	14.28 (2)	50.0 (7)

*all values reported as %(n)

PDL-1 status was significantly correlated to an improved clinical stage (p= 0.0277).

Conclusions: Recent findings indicate that STAT-1 and STAT-3 stimulate PD-L1 expression in HNSCC. In this cohort, we found that PD-L1 weakly positively correlates to STAT-1 expression on a protein level. These findings are concordant with the The Cancer Genome Atlas (TCGA) findings that PD-L1 correlates to STAT-1 expression on a molecular level. Similar to previous findings, PDL-1 is more intensely expressed on p16-positive HNSCC and is associated with improved clinical prognosis.

1330 PD-L1 Expression Predicts Improved Disease Free Survival in High Risk Head and Neck Cutaneous Squamous Cell Carcinoma

Edward Roper, Trina Lum, Carsten E Palme, Bruce Ashford, Sydney Ch'ng, Marie Ranson, Michael Boyer, Jonathan Clark, Ruta Gupta. Royal Prince Alred Hospital, Sydney, NSW, Australia; Chris O'Brien Lifehouse, Sydney, NSW, Australia; University of Sydney, Sydney, NSW, Australia; University of Wollongong, Wollongong, NSW, Australia; Illawarra Health and Medical Research Institute, Wollongong, NSW, Australia; Illawarra and Shoalhaven Local Health District, Wollongong, NSW, Australia; Centre for Oncology Education and Research Translation, Liverpool, NSW, Australia; University of New South Wales, Sydney, NSW, Australia.

Background: Programmed cell death (PD-1) and its ligand (PD-L1) inhibitors have shown clinical response in many tumors. The data regarding PD-L1 is limited and no clinical trials are published for PD-1/PD-L1 inhibitors in head and neck cutaneous squamous cell carcinoma (HNcSCC).

Design: We aimed to evaluate PD-L1 expression in high risk HNcSCC, clinicopathological associations, prognostic significance, and heterogeneity in matched metastases. 74 primary cases were included, 38 having metastases.

Results: We observed PD-L1 expression in >5% of primary tumor cells in 29 cases (39.2%), primary tumor infiltrating lymphocytes (TILs) in 40 cases (70.2%), metastatic tumor cells in 15 cases (39.5%), and metastatic TILs in 18 cases (47.4%). PD-L1 expression in >5% of primary tumor cells was associated with an inflammatory phenotype (p=0.04), and in primary TILs with clear margins (p=0.05). PD-L1 expression in >5% of primary tumor cells (p=0.01), primary TILs (p=0.001), and metastatic TILs (p=0.02) was associated with improved disease free survival. PD-L1 expression in >5% of tumor cells was heterogeneous between primary and metastatic tumors in 13 cases (34.2%).

Conclusions: PD-L1 expression is common in HNcSCC supporting the rationale for a clinical trial of PD-1/PD-L1 inhibitors. PD-L1 expression in tumor cells or TILs predicts improved disease free survival, and demonstrates tempero-spatial heterogeneity.

1331 Comprehensive Genomic Profiling of Metastatic Salivary Gland Cancer

Jeffrey Ross, Julia A Elvin, Jo-Anne Vergilio, James Suh, Shakti H Ramkissoon, Kai Wang, Daniel Bowles, Hilary Somerset, Siraj M Ali, Alexa Schrock, David Fabrizio, Garrett Frampton, Vincent Miller, Philip Stephens, Laurie M Gay. Albany Med Col, Albany, NY; Foundation Med, Cambridge, MA; Univ of Colorado, Denver, CO.

Background: Using comprehensive genomic profiling (CGP) we compared histologic subtypes and searched for clinically relevant genomic alterations (CRGA) linked to targeted and immunotherapies for patients with relapsed and metastatic salivary gland carcinomas (mSGC).

Design: DNA was extracted from 40 microns of FFPE from 454 cases of mSGC. CGP was performed on hybridization-captured, adaptor ligation based libraries to a mean coverage depth of >600X for up to 315 cancer-related genes plus 37 introns from 14 genes frequently rearranged in cancer. Tumor mutational burden (TMB) was calculated as mutations/Mb by counting the number of synonymous and non-synonymous mutations across a 1.11 Mb region.

Results: The more differentiated mSGC (ACC, AciCC, MyC, MASC) have significantly lower frequencies of GA, TP53 mutations, targetable GA and TMB than the less-differentiated mSG (MEC, DCA, AC-NOS, CA-NOS, CPA). The less-differentiated CA are frequently *ERBB2* driven tumors, but also harbor *RET*, *BRAF* and *NF1* targets and feature higher TMB that will be shown to be responsive selected precision therapies.

Tumor Type/ cases	GA/ Tumor	Notable GA	TP53 GA	ERBB2 GA	RET/ BRAF GA	TMB≥10 mut/Mb
AdenoidCystic Carcinoma (ACC)/154	1.6	MYB-NFIBFGFR1 CDK4	4%	0%	0%/0%	1%
AcinicCell Carcinoma (AciCC)/67	2.8	PTEN BRAF	10%	0%	0%/3%	3%
Myo-epithelial Carcinoma* (MyC)/24	3	RICTORPTCH1PDGFRB	13%	0%	0%/0%	5%
MammaryAssociated Secretory Carcinoma (MASC)/16	2.8	ETV6-NTRK3 (100%)#	13%	0%	0%/0%	0%
Muco-epidermoidCarcinoma (MEC)/46	4.0	PIK3CAERBB2BRCA2	43%	9%	0%/2%	10%
DuctalCarcinoma (DCA)/41	3.6	ERBB2 RET NF1 BRAF	54%	27%	5%/5%	11%
Adeno-Carcinoma NOS(AC-NOS)/50	3.9	ERBB2BRAFRET	56%	15%	2%/6%	6%
Carcinoma NOS(CA-NOS)/32	5.2	ERBB2 NF1	59%	19%	0%/0%	13%
Carcinoma ex Pleomorphic Adenoma (CPA)/24	3.0	ERBB2	46%	29%	0%/0%	12%

*Includes 3 cases of CPA #Highly targetable *NTRK* fusions not present in any other subtype

Conclusions: mSGC include classic differentiated carcinomas (ACC, AciCC, MyC, MASC) with low GA frequencies, low TMB and limited opportunities for both targeted and immunotherapies. The less-differentiated mSG (MEC, DCA, AC-NOS, CA-NOS, CPA), feature higher GA frequencies, targeted therapy opportunities for HER2, RET, BRAF and MTOR inhibitors and higher TMB guiding the use of immune checkpoint inhibitors.

1332 Perineural Spread in Lymphomas of the Head and Neck

Ana Ruano, Mihai Merzianu. Roswell Park Cancer Institute, Buffalo, NY.

Background: Perineural invasion, histological (invasion; PNI) or radiologic (spread; PNS), an independent prognostic factor in head and neck carcinoma (HNCA), has been described as a feature to discriminate salivary gland extranodal marginal zone lymphoma (ENMZL) from benign lesions (LESA). Rare case reports of PNI/PNS in head and neck lymphomas (HNL) exist but no systematic studies have assessed its frequency, distribution and clinical significance.

Design: 67 HNL, 10 gland lymphoproliferations and 10 lymphomas with reported PNI (including 5 HNL) were studied. PNI was reviewed by 2 observers, defined as tumor involving >33% of extratumoral nerve circumference or with concentric lamination or intraneural infiltration of intratumoral nerves (Liebig *et al*, 2009). Number & size of involved fibers, distance to main tumor, and angiotropism were recorded. Clinical-radiology findings were available in 69 cases. Chi-square and t-test statistics were used.

Results: Lymphomas were of B (n=69) and T (n=8) lineage, from 32 men & 45 women with median age of 61 yr (26-88). Most common HNL were follicular (n=21), DLBCL (n=20), and ENMZL (n=13) from parotid (n=27), cervical lymph nodes (n=16), submandibular gland (n =11), and oropharynx (n=8). Of 53 lymphomas with identifiable nerve fibers, 30 (57%) had PNI (16 aggressive, 14 indolent); 3 (10%) had neurologic symptoms and 4 (17%) showed PNS. PNI (>3 fibers) was extensive in 23 (77%); 13 (43%) had both intra and extratumoral PNI, mostly in small (<1 mm) fibers (n=22, 73%); and 16 (53%) showed angiotropism. 10 (42%) had recurrences, 7 loco-regionally, none involving CNS. In lymphomas without PNI (n=23) (11 aggressive, 12 indolent), 6 (30%) recurred, 2 (10%) loco-regionally, but none had neurologic symptoms or PNS. Only 5 (22%) showed angiotropism. Among cases without nerve fibers (n=24), 2 (8%) had neurologic symptoms and 3 (12%) PNS. No benign lesions showed PNI, angiotropism, neurologic symptoms or PNS. No significant difference in demographic/clinical characteristics was found between PNI+ and PNI- HNL, but the PNI+ group showed a trend for locoregional recurrence ($p=0.08$) and a significant correlation with angiotropism ($p<0.05$). PNI was detected in 21/67 (31%) HNL at re-review but documented only in 5/72 (7%) HNL reports.

Conclusions: PNI is a common, underreported finding in HNL, difficult to diagnose due to diffuse disease and ill-defined borders, requiring stricter criteria than in HNCA. It associates with angiotropism and is not seen in benign conditions. PNI in HNL may represent a locoregional spread pathway and should be reported. Whether it reflects true neurotropism is unclear.

1333 p16 Expression in Cutaneous Squamous Cell Carcinoma (cSCC) of the Head and Neck

Laveniya Satgunaseelan, Hyerim Suh, Sohaib Virk, Bruce Ashford, Trina Lum, Marie Ranson, Jonathan Clark, Ruta Gupta. Royal Prince Alfred Hospital, Sydney, NSW, Australia; University of New South Wales, Sydney, NSW, Australia; University of Wollongong, Wollongong, NSW, Australia; Illawarra Health and Medical Research Institute, Wollongong, NSW, Australia; Illawarra Shoalhaven Local Health District, Wollongong, NSW, Australia; University of Sydney, Sydney, NSW, Australia; Chris O'Brien Lifehouse, Sydney, NSW, Australia.

Background: Metastatic squamous cell carcinoma of unknown primary is a common presentation in the neck. p16 expression, as determined by immunohistochemistry, is often used as a surrogate marker of human papillomavirus infection and an indicator of an oropharyngeal primary. Australia has the highest rate of cutaneous SCC (cSCC) in the world, with head and neck cSCC (HNcSCC) being known to present with cervical metastases. p16 expression in HNcSCC is yet to be elucidated. The objective of the study was to evaluate the incidence of p16 expression in HNcSCC and analyse its association with conventional prognostic factors and survival outcomes.

Design: p16 immunohistochemistry was performed on tissue micro-arrays of 166 patients in the Sydney Head and Neck Cancer Institute database with HNcSCC (2000-2013) and on whole sections (n=51) following histopathology review.

Results: 53 (31.9%) cases showed strong, diffuse nuclear and cytoplasmic p16 expression. p16 expression significantly increased with increasing histological grade ($p=0.005$). No significant difference was seen in the rate of nodal involvement (p16 positive – 73.1% vs. p16 negative – 81.7%, $p=0.21$), extranodal spread (p16 positive – 22.6% vs. p16 negative – 26.5%, $p=0.59$), or other conventional histopathological parameters. p16 expression was not associated with disease-specific or disease-free survival.

Conclusions: p16 expression is seen in nearly 32% of HN </del>cSCCs, particularly poorly differentiated HNcSCC. Thus HNcSCC should also be considered during the evaluation of squamous cell carcinoma of unknown primary in the neck, particularly in the regions with high prevalence of HNcSCC.

1334 Beyond the Percentages of PD-L1-Positive Tumor Cells: Induced versus Constitutional PD-L1 Expression in Primary and Metastatic Head and Neck Squamous Cell Carcinoma

Theresa Scognamiglio, Yao-Tseng Chen. Weill Cornell Medical College, New York, NY.

Background: Immune checkpoint blockade with anti-PD1 antibody has been FDA-approved for treating metastatic head and neck squamous cell carcinoma (HNSCC) and an objective response rate of 18-20% has been reported. Defining PD-L1 expression at >1% tumor cells as positive, PD-L1-positive tumors showed higher response rate, suggesting PD-L1 as a predictive marker. However, it is unclear whether 1% is the optimal cutoff, and studies on lung cancer have suggested 50% cutoff as a stronger predictor of clinical response. Studies to correlate PD-L1 expression to HPV status were inconclusive, and correlations between primary and metastatic lesions have not been done.

Design: 95 primary HNSCC from oropharynx and oral cavity were typed for membranous PD-L1 expression. 34 corresponding metastatic lesions were also tested. HPV status was determined by in situ hybridization or p16 as a surrogate marker.

Results: 29 of 95 (31%) showed no PD-L1 expression. 35 (37%) showed induced expression at the tumor-immunocyte interface, either in immunocytes--lymphocytes and histiocytes--only (N=12) or in immunocytes and adjacent tumor cells (N=23). The remaining 31 (33%) showed constitutional expression in tumor cells beyond interface, including 21 in 5-50% of tumor cells and 10 (11% of all cases) in >50% of tumor cells (Figure 1).

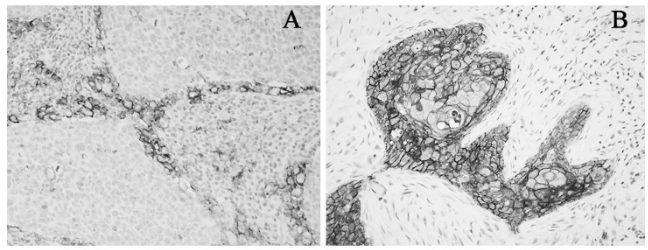

Fig.1 Induced (A) and constitutional (B) expression of PD-L1 in HNSCC

Of the 34 primary-metastasis tumor pairs, PD-L1 expression was concordant in only 18 pairs (53%), whereas 8 cases each showed an up or down PD-L1 expression in metastasis. Most of these differences reflected changes in the induced expression, but not the constitutional expression.

Among HPV(+) cases, 54% (22/41) showed induced PD-L1 expression, significantly more frequent than in the HPV(-) cases (13/54, 24%, $p=0.03$), likely reflecting their stronger immunogenicity. In contrast, both HPV(+) and HPV(-) had similar frequency of constitutional PD-L1 expression (34% vs. 32%).

Conclusions: HNSCC could show constitutional PD-L1 expression or be induced to express PD-L1 at the tumor-immunocyte interface. Distinguishing these two patterns of expression and typing metastatic lesions before treatment might better predict clinical response to anti-PD1 (or anti-PD-L1) beyond the percentage of PD-L1-positive tumor cells.

1335 MiRNA-200c and MiRNA-141 as Epithelial Mesenchymal Transition Regulators and Novel Potential Biomarkers in Eyelid Sebaceous Gland Carcinoma

Seema Sen, Mansi Bhardwaj, Kunzang Chosdol, Anjana Sharma, Neelam Pushker, Mandeep S Bajaj, Sameer Bakhshi, Seema Kashyap. Dr R.P Centre, AIIMS, New Delhi, India; AIIMS, New Delhi, India.

Background: Sebaceous gland carcinoma (SGC) is the most common malignant eyelid tumor in Asian countries with a high rate of recurrence and metastasis. Invasion and metastasis in various carcinomas is promoted by activation of epithelial-mesenchymal transition (EMT). EMT is characterized by downregulation of miRNA-200c and miRNA-141, which leads to transcriptional repression of E-cadherin gene. The present study was performed to determine the status of miRNA-200c and miRNA-141, their association with E-cadherin and clinicopathological features.

Design: Prospective analysis of 42 eyelid SGC patients was undertaken. Clinicopathological features, including Hematoxylin & Eosin stained sections of FFPE tumors were reviewed to confirm the diagnosis. AJCC staging was done according to 2009 guidelines. Patients were followed up for a period of 7-44 months. miRNA-200c, miRNA-141 and E-cadherin expression were determined in all the tumour samples and adjoining normal skin tissues by quantitative Real Time PCR (qPCR) using Taqman miRNA assay and SYBR Green Chemistry (Applied Biosystems) respectively. Their association with E-cadherin was also determined by immunohistochemistry (IHC). Results were correlated with high risk features and follow up data. Kaplan-Meier plots and Spearman's rank correlation tests were applied to analyze the data.

Results: The mean age of patients was 58.7 ±1.3 years with male: female ratio of 0.9:1. Low expression of miRNA-200c and miRNA-141 were seen in 36/42 (86%) and 28/42 (67%) cases respectively. Low E-cadherin expression was observed in 28/42 (67%) and 27/42 (64%) by IHC and qPCR respectively. Low miRNA-200c correlated significantly with advanced tumor stage (P= 0.05), large tumor size (P= 0.03) and poor differentiation (P = 0.03). Low miRNA-141 correlated significantly with large tumor size (P= 0.02) and lymph node metastasis (P= 0.04). Survival analysis revealed that patients with low miRNA-200c (P= 0.05) had significant shorter disease-free survival. There was a significant association of both miRNA-200c (P= 0.006) and miRNA-141 (P= 0.002) with E-cadherin expression.

Conclusions: Low levels of miRNA-200c and miRNA-141 in eyelid SGC patients promotes EMT by E-cadherin repression and miRNA-200c has emerged as a novel potential predictor of survival.

1336 NKX3.1 Is a Marker of Salivary Duct Carcinoma (SDC)

Gabriel Sica, Cynthia Cohen, Christopher C Griffith. Emory University, Atlanta, GA.

Background: Previous studies have shown that NKX3.1 is a very sensitive and specific marker for prostatic carcinomas, especially in the metastatic setting. Since NKX3.1 is a protein that is expressed primarily in the prostate and salivary glands and SDC expresses proteins that are normally expressed in prostatic carcinomas, we investigated whether SDC would be one of the few tumor types in addition to prostatic carcinoma that would express NKX3.1.

Design: 22 SDC or SDC ex pleomorphic adenoma (EXPA) were immunohistochemically stained for NKX3.1. Any nuclear staining was considered positive for NKX3.1.

Results: There were 16 SDC and 6 SDC EXPA with 16 males and 6 females ranging in age from 41-84 years (median 72.5 years). The majority of the tumors originated in the parotid gland (n=17) with the remainder originating in the submandibular gland (n=3), sinonasal/lacrimal gland (n=1) and parapharyngeal space (n=1). Immunohistochemical staining for NKX3.1 in SDC/SDC EXPA showed that NKX3.1 is expressed either in a patchy distribution or as focal scattered cells. 36% of SDC/SDC EXPA expressed NKX3.1 with the majority (7 of 8) of the NKX3.1 positive cases being pure SDC.

Conclusions: NKX3.1 is expressed in a significant fraction of SDC and could be a useful diagnostic aid in the setting of metastatic SDC. In addition, this study expands the very few tumor types (prostatic and breast lobular carcinoma) that are known to express NKX3.1.

1337 An Update in the Risk of Lymph Node Metastasis for the Follicular Variant of Papillary Thyroid Carcinoma with the New Diagnostic Paradigm

Aleksandra Sowder, Benjamin L Witt. University of Utah, Salt Lake City, UT.

Background: Papillary thyroid carcinoma (PTC) accounts for approximately 85% of all thyroid cancers. The majority of PTCs are either the classical or follicular variant. Previous data has shown that the risk of nodal metastases is significantly greater for classical PTC as compared to the follicular variant. The recent reclassification of encapsulated follicular variant of papillary thyroid carcinoma (FVPTC) to a non-malignant tumor [noninvasive follicular thyroid neoplasm with papillary-like nuclear features (NIFTP)] limits the category of FVPTC to the invasive subtype only. Given this change in diagnostic paradigm, we intend to investigate if there remains a significant difference in nodal involvement between classical PTC and the follicular variant of PTC.

Design: A 6 year retrospective review (from 1/1/2010 to 12/31/2015) of all cases with FVPTC in the diagnostic line from the University of Utah/ARUP Laboratories was conducted, identifying a total of 127 cases. Forty-four cases that had both a classical PTC and a FVPTC component were eliminated from the histologic review component of the study. Two pathologists reviewed the remaining cases using the recently described histologic criteria of NIFTP to determine the total number the FVPTCs fitting the new classification paradigm. Histologic and clinical follow-up was tracked for all patients to determine the rate of nodal disease for all groups.

Results: One hundred and twenty-seven cases were identified using the above listed criteria. Forty- seven cases (37%) were classified as NIFTPs based on the newly-defined diagnostic parameters. None of the 47 patients had nodal disease either at the time of surgery or on follow-up (a lymph node excision was performed in 13 cases). Twenty-eight cases met the current criteria for FVPTC (21%); of these 7/28 (25%) had evidence of nodal disease (a lymph node excision was performed in 17 cases). By comparison, 17/45 (38%) of patients with mixed classical and FVPTC had nodal disease (a lymph node excision was performed in 29 cases). Overall, there was no statistically significant difference in the risk of nodal metastasis between the pure FVPTC and mixed classical/FVPTC groups (p=0.43).

Conclusions: Our data indicates that implementing new definition for FVPTC will narrow the gap in the risk of nodal metastases between the classical PTC and FVPTC histologic subtypes. This suggests that other risk parameters, such as tumor size and extra-thyroidal extension play a more significant role than histologic subtype in determining risk of nodal involvement in PTC.

1338 Thirty-Nine Cases of Sinonasal Tract Alveolar Rhabdomyosarcoma in Adults

Lester DR Thompson, Vickie Y Jo, Abbas Agaimy, Antonio Llombart-Bosch, Gema N Morales, Isidro Machado, Markku M Miettinen, Justin A Bishop. SCPMG, Woodland Hills, CA; Brigham & Women's Hosp, Boston, MA; Universitasklinikum Erlangen, Erlangen, Germany; Univ. of Valencia, Valencia, Spain; Inst. de Oncologia, Valencia, Spain; NIH, Bethesda, MD; Johns Hopkins Med Inst., Baltimore, MD.

Background: Sinonasal tract (SNT) alveolar rhabdomyosarcoma (ARMS) are frequently misdiagnosed, especially in adults.

Design: 39 adult patients with SNT ARMS were reviewed, immunohistochemistries performed and molecular studies tested.

Results: 21 females and 18 males (18 to 72; mean, 42.8 yrs), presented for a short duration (mean, 2.5 mo) with a large (mean, 6.0 cm) destructive nasal mass, involving multiple sites (n=34) and with cervical adenopathy (n=28). An alveolar, nested to solid growth below an intact, but often affected (n=6) epithelium showed necrosis (n=26), bone invasion (n=25), and lymphovascular invasion (n=25). The neoplastic cells were dyscohesive and dilapidated, with crush artifacts. Rhabdoid features (n=34) and tumor cell multinucleation (n=28) were common. Mitotic counts were high (mean, 22/10 HPFs). The neoplastic cells showed the following IHC:

Antigen	Result	%/# of Cases
Desmin	P,S,D,C	100% (39/39)
Myogenin	P,S,D,N	100 % (37/37)
MyoD1	P,S,D,N	100% (21/21)
Actin (HHF35)	P,S,D,C	94% (17/18)
Actin-SM	P,S,D,C	36% (8/22)
Cytokeratin	P,W-S,F-D,C-T	36% (13/36)
CAM5.2	P,W-S,F-D,C-T	51% (19/37)
CK5/6	P,S,D,T	5% (1/22)
S100 protein		25% (9/36)
CD56	P,S,D,M	100% (26/26)
Synaptophysin	P,W-S,F-D,C	36% (14/39)
Chromogranin	P,W,F,C	22% (8/37)

(P-positive; S-strong; D-diffuse; F-focal; C-cytoplasmic; N-nuclear; W-weak; T-dot; M-membrane)

Molecular studies showed *FOXO1* translocations (n=9); PCR pending. Patients presented with high stage (IV: 22; III: 14) and metastatic disease (n=33). Surgery (n=11), radiation (n=30) and chemotherapy (n=33) yielded an overall survival of 40.5 mo (mean 2.4–286); 22 have disease (mean 17.3); 15 alive without disease (mean 72.9); 6 alive with disease (mean 8.8); 1 dead without disease (63.7); 16 dead with disease (mean 20.5).

Conclusions: SNT ARMS frequently present in adults as a large, destructive midline mass of short symptom duration, with high stage disease. The alveolar to solid pattern of growth of cells with rhabdoid-plasmacytoid cells supports the diagnosis. Epithelial and neuroendocrine markers are frequently present, leading to misdiagnosis if muscle markers are not performed. Overall survival of 40.5 mo is achieved with multimodality therapy, but 56% have incurable disease (17.3 mo).

1339 Circulating Cell Free DNA Levels in Oral Squamous Cell Carcinoma

Vandana Tiwari, Sudaiv Nagzarkar, Abhinav A Sonkar, Swati Kumari, Nuzhat Husain. Dr. Ram Manohar Lohia Institute of Medical Sciences, Lucknow, Uttar Pradesh, India; King George's Medical University, Lucknow, Uttar Pradesh, India.

Background: Oral squamous cell carcinoma (OSCC) represents the sixth prevalent malignancy worldwide and the third most common cancer in developing countries (1, 2). Estimation of Circulating free DNA may serve as non-invasive biomarker for detection of OSCC in an early stage. The present study was designed to assess serum cfDNA level in OSCC as compared to normal control.

Design: Serum sample was collected from 44 patients with OSCC (Stage I=4, II=16, III=15, IV=9) and 20 healthy individuals. DNA was isolated by commercially available Kit. CfDNA levels were quantified by quantitative SYBR Green real-time PCR through amplification of β-globin gene.

Results: Mean (±SD) cfDNA level was significantly higher in OSCC cases (317.42±392.47; range 10.508 - 1566.28) as compared to normal controls (68.12±64.17; range 8.75 - 218.55 p=0.004).Serum cfDNA levels were significantly associated with TNM stage III and IV patients and lymph node involvement (p= 0.004 & 0.0001 respectively). However, cfDNA levels did not correlate with histological grade of the patients. Association of cfDNA level with demographic and clinicopathological characterstics of the patients is summarized in Table 1.

Characterstics	N	cfDNA (ng/ml)	p Value
Age (yrs) ≤45 >45	 21 23	 263.56 ± 313.01 332.92 ± 433.37	0.549
Sex Male Female	 33 11	 288.37 ± 372.65 404.55 ± 454.79	0.401
Stage I + II III IV	 20 15 09	 195.23 ± 289.92 287.23 ± 365.98 639.26 ± 488.21	0.004
Lymph Node Involvement Present Absent	 15 29	 658.03 ± 396.20 141.24 ± 252.52	0.0001
Histological Grade Well Differentiated Moderately differentiated Poorly differentiated	 15 17 12	 384.92 ± 515.17 298.28 ± 327.97 260.15 ± 312.30	0.468

Conclusions: Quantitative analysis of cfDNA may distinguish Oral Squamous Cell Carcinoma cases from normal control and appears to be promising biomarker for non invasive detection of malignancy.

1340 Does the Extent of Extracapsular Spread in Lymph Node Metastases Correlate with Outcomes in Oropharyngeal Squamous Cell Carcinoma? – A Retrospective Study

Beena Umar, Steve Chang, Tamer Ghanem, Farzan Siddiqui, Gordon Jacobsen, Derek Isrow, Christian E Keller. Henry Ford Hospital (HFH), Detroit, MI.

Background: Extracapsular spread (ECS) in lymph node (LN) metastases of Head and Neck squamous cell carcinoma (SCC) is an accepted poor prognosticator with higher rates of regional recurrence and distant metastasis. As such, ECS is an important criterion guiding therapy. Most ECS studies do not take into account anatomic subsites. Oropharyngeal SCC (OSCC) is linked to HPV infection, affects non-smokers, younger patients and has a favorable treatment response. Currently, the impact of ECS extent (ECSE) on disease outcome, if any, is not well established.

Design: We reviewed 92 OSCC of patients who underwent surgery as initial treatment at HFH from 1994 to 2015. ECSE was stratified as follows: ECS 0: intact lymph node capsule (LNC); ECS I: limited breach of and measureable extension beyond the LNC, ECS II: morphologically distinct and partly coalescing metastatic nodules that form a mass maintaining a fibrous (pseudo-)LNC; ECS III: SCC diffusely infiltrating neck structures such as fibroadipose or muscle tissue, nerves and vessels. Kaplan-Meier survival curves were used to estimate disease free survival (DFS) and overall survival (OS). Cox-regression analysis was used to examine the impact of ECSE on DFS and OS while adjusting for p16 and smoking status. Cochran-Armitage Trend Test was used to explore a possible association of ECSE and race, alcohol use, margin status and largest lymph node size.

Results: Our cohort comprised 77 (84%) men and 15 (16%) women with a mean age of 60.1 years (SD 9.1). In 3.1 years of average follow (0.1- 9.3 years), 14 patients died, 5 recurred and 9 developed metastases. After review, patients were grouped as follows: 45 ECS 0, 9 ECS I, 7 ECS II, 12 ECS III and 18 lymph node negative patients. The study group comprised 70 (76%) patients with overexpression of *TP16* protein, 23 never-smokers and 64 smokers (current and past). ECS III was associated with poor DFS ($p=0.002$) and OS ($p<0.001$) in Kaplan-Meier survival analysis. When adjusted for p16 and smoking status the correlation between ECS III and PFS ($p<0.001$) / OS ($p<0.001$) was retained in Cox Regression modeling. African Americans were more frequent in ECS III (0.021) while Caucasians were more frequent in non-ECS III groups ($p=0.026$). ECSE did not correlate with alcohol use ($p=0.224$), margin status ($p=0.315$) or nodal metastasis size ($p=0.717$).

Conclusions: In our cohort, only ECS III is correlated with poor DFS and OS in OSCC when adjusted for p16 status and smoking.

1341 Matlab Silhouette Analysis of Worst Pattern of Invasion in Oral Squamous Carcinomas

Minhua Wang, Lei Zhang, John E Tomaszewski, Scott Doyle, Margaret Brandwein. State University of New York, Buffalo, NY.

Background: Machine classifiers are advantaged over pathologist-based classification schemas in the unlimited ability to query a huge number of variables. The prior knowledge that tumor dispersion (Worst pattern of invasion type 5, or WPOI-5) is a validated outcome predictor for oral squamous cell carcinoma (OSCC) is leveraged for image analysis of silhouettes generated from T1/T2 OSCC with WPOI-5 or WPOI-4.

Design: 25 slides from 15 patients withT1/T2 OSCC were scanned at high-resolution (8 WPOI-5 and 7 WPOI-4). Carcinoma and satellites were annotated to create "ground truth" silhouette images. Based on each silhouette image, Delaunay triangulation was generated and 51 texture-based features were extracted, such as size, shape and distance. Statistics were applied to select the features for maximum relevance to distinguish nonaggressive from aggressive pattern of invasion. In addition, these manual annotation silhouette images set up training sets. Machine learning classifiers were established using these "ground truth" silhouette images to identify tumors.

Results:

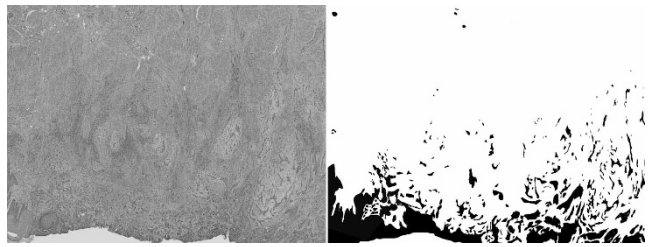

Fig 1 (left) shows an OSCC with scattered tumor satellite invasion. (Right) illustrates a "ground truth" silhouette image with the dispersed tumor satellites easily appreciated.

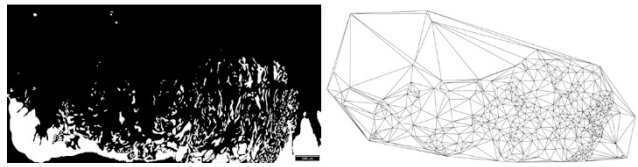

Fig 2 (left) shows a silhouette image. (Right) illustrate a Delaunay triangulation based on the left silhouette image.

Conclusions: We present proof of assumption that computer based image analysis can envision WPOI in oral squamous cell carcinoma based on the interpretation of digitalized images.

1342 A Novel Approach to Evaluating Frozen Sections for Acute Invasive Fungal Sinusitis

Bartholomew White, Joshua I Warrick, Jaccob Hodos, Max Hennessy, Sakeena Payne, John McGinn, David Goldenberg, Henry Crist. Penn State Hershey Medical Center, Hershey, PA.

Background: Frozen sections (FS) are routinely utilized in the rapid diagnosis of acute invasive fungal sinusitis (AIFS), yet FS interpretation can be diagnostically challenging in a significant number of patients. Difficulty in recognizing this potentially fatal illness results from the inherent aspects of the sinonasal tissue and characteristics of fungi in AIFS. Although some of the morphologic features of fungi and the tissue's reaction are well known, a detailed morphologic description has not been published in the literature. Recognition of these details at the time of FS may improve diagnostic sensitivity and specificity leading to better patient outcomes.

Design: A retrospective review conducted of all FS performed for suspected AFIS at our institution from 2006 to 2016 yielded 218 biopsies including 49 positive and 169 negative biopsies. The FS slides were collected, blinded, and reviewed. Distinct morphologic changes were recorded and the results were compared to the permanent H&E sections and Grocott Metamine Silver stains for diagnostic accuracy. Features which hindered or caused false interpretation were recorded as pitfalls. A 30 minute periodic acid Schiff (PAS) stain was developed to aid in diagnosing AIFS as well.

Results: Forty-nine biopsies showed AIFS and were recorded as positive. In positive cases the characteristic finding was necrosis (85%) which appeared as a coagulative-like change or as a mucinous or loose fibrinous-like network with loss of identifiable structures. Vascular fungal thrombosis (VFT) present as hyphae plugging vessels was frequently seen within the necrosis (61%). This characteristic necrosis and VFT were present only in the positive cases, while surface necrosis/ulceration was present in both positive and negative cases. Avoidance of specific pitfalls in fungus identification (collagen fibers, fibrin strands, thin vascular walls, slits, vacuolated spaces, tissue and mucus folds, etc.) improved accuracy in frozen section interpretation. The concurrent development of a rapid 30 min PAS FS procedure showed potential in demonstrating fungal walls not otherwise visible.

Conclusions: AIFS frequently displays characteristic morphologic changes such as specific necrosis patterns and VFT at the time of FS. There are benign mimics of AFIS, but knowledge of these pitfalls facilitates a more accurate diagnosis. In addition, supplementing the FS with the use of a novel rapid modified PAS stain in these sensitive cases can supply prompt information critical to patient care.

1343 Salivary Gland Epithelial Neoplasms in the Pediatric Population: A Single Institute Experience with a Focus on the Histologic Spectrum

Bin Xu, Amandeep Aneja, Ronald Ghossein, Nora Katabi. Memorial Sloan Kettering Cancer Center, New York, NY.

Background: Salivary gland epithelial neoplasms are rare in children and adolescents and only a handful of large series have been published to date. In this study, we aimed to characterize the clinicopathologic spectrum of these tumors.

Design: A retrospective clinicopathologic review was conducted for 56 cases operated at our center between 1992 and 2016 in patients that were 20 years or younger.

Results: The patients' age ranged from 4-20 years (29 females and 27 males). The tumors were located in the parotid (n=36), submandibular gland (n=7), and minor salivary glands (n=13). 19 (34%) tumors were benign being pleomorphic adenoma, while the remaining (66%) were malignant. The histologic types of carcinomas were as follows: mucoepidermoid carcinoma (MEC, n=19, 34%), acinic cell carcinoma (n = 7, 13%), adenoid cystic carcinoma (n = 6, 11%), mammary analog secretory carcinoma (MASC, n = 4, 7%), and myoepithelial carcinoma (n = 1, 2%). 92% (12/13) of the minor and 58% (25/43) of the major salivary gland tumors were malignant. The majority of MECs were intermediate grade (16/19, 84%). Among the 46 patients with

available clinical FU (median = 52 months), a seven-year girl (2%) with a high grade MEC suffered of disease-related death due to uncontrollable locoregional recurrence. Seven patients (17%) developed recurrence including 2 distant metastases from adenoid cystic carcinoma and 6 locoregional recurrences (2 pleomorphic adenomas, 1 MASC, 1 myoepithelial carcinoma, 1 adenoid cystic carcinoma, and 1 MEC). The following parameters were associated with decreased disease free survival: elevated mitotic index of > 4/10 HPFs (log rank test, $p < 0.001$), advanced AJCC pT ($p = 0.029$) and pN stage ($p < 0.001$).

Conclusions: 1) Two third of pediatric salivary gland epithelial neoplasms are malignant, with MEC being the most common malignant tumor.

2) Myoepithelial carcinoma and MASC can occur in the pediatric population and should be considered in the differential diagnosis.

3) Compared to adults, salivary gland malignancies in children appear to have better clinical outcome, associated with 5% nodal metastasis, 7% distant recurrence, 13% locoregional recurrence, and a 10-year disease specific survival of 94%.

1344 Warthin's Tumor: A Study of 73 Cases with Emphasis on Association with Other Malignancies

Daniel Zaccarini, Kamal K Khurana. SUNY Upstate Medical University, Syracuse, NY.

Background: Warthin's tumor, the second most common benign parotid gland neoplasm, is frequently diagnosed on aspiration cytology. Its association with non-salivary gland neoplasms has been sporadically reported. We reviewed clinical records of Warthin's tumor diagnosed on aspiration cytology and surgical pathology to determine if there was any association with other extra salivary gland malignant neoplasms.

Design: Computer search was made for all cases of Warthin's tumor diagnosed in the parotid gland by aspiration cytology and surgical pathology at our institution between January 2007 and August 2016. Clinical records of all cases were reviewed for any associated neoplasms and any surgical follow up. All cytology and histologic material was reviewed. Statistical analysis was performed using student T test.

Results: Age of patients ranged from 43 to 87-years (mean 66.9, M:F 1.1:1). Twenty-seven (37.0%) patients harbored a malignant neoplasm [squamous cell carcinoma(9), basal cell carcinoma(3), lung adenocarcinoma(3), renal cell carcinoma(2), breast carcinoma(2), melanoma(2), lymphoma(2), prostate adenocarcinoma(1), oligoastrocytoma(1), thyroid carcinoma(1), and cholangiocarcinoma(1)]. Aspiration cytology in all cases revealed oncocytes and lymphocytes. Surgical pathology follow-up available in 19 of 60 (31.2%) aspirates showed 100% concordance with cytology diagnosis. Average age for patients with and without secondary malignancy was 70.5-years, and 63.4-years, respectively ($p < 0.05$). Average pack years for patients with and without secondary malignancy was 45.4, and 39.8, respectively ($p > 0.05$). 54(74.0%) cases presented with palpable lesions, 10(13.7%) were discovered on PET scan (SUV> 4.2), 8(11%) were detected by CT, and 1(1.3%) by MRI.

Conclusions: Association of extra salivary gland malignant neoplasm in 37.0% of our cases suggest that the prevalence of secondary neoplasms in patients harboring Warthin's tumor might have been underestimated. Squamous cell carcinoma was the most commonly associated malignant neoplasm. Caution is warranted in interpretation of PET scans commonly used to assess for metastatic disease in patients as increased SUV in Warthin's tumor may be mistaken as evidence for metastatic disease.

1345 Cancer Gestalt: Fused Cancer and Biomarkers in Three-Dimensions-A Novel Way to Envision Tumor Biology

Lei Zhang, Jing He, Poojaben Dhorajiya, Minhua Wang, Scott Doyle, Margaret Brandwein. SUNY at the University at Buffalo, Buffalo, NY.

Background: Pathologists experientially identify and quantify disease processes by interpreting planar images (glass slides) correlated with other data to arrive at three dimensional (3D) mental imagery (or gestalt) of complex processes. We believe that concrete 3D modeling of tissue morphology colocalized with biomarkers has the potential to enhance our understanding of diseases. Worst pattern of invasion (WPOI) represents specific architecture at the cancer/non-cancer interface. This classification is based solely on 2D planar analysis of complex 3D structures. Possibly, important diagnostic information may be better revealed in a fully 3D model. As proof of principal, we selected two biomarkers (CD44v6 and ALDH1) which have been previously demonstrated to be related to cancer invasion and stemness.

Design: Paraffin embedded tissue blocks of 8 cases of oral cavity cancers (WPOI-5 versus nonaggressive invasion) were sectioned to obtain 180 4-um consecutive sections. H&E stain was performed on every other section out of 180 sections. The blanks in between each H&E sections were stained for CD44 v6 and ALDH1 by immunohistochemistry (IHC). Slides were digitalized with an Olympus scanner at 40x, and processed in Photoshop, FIJI, Matlab, and Meshlab for 3D reconstruction.

Results: Our initial analysis of two cases with different WPOI grades clearly showed distinct microarchitecture of the tumor front in the 3D models. Overlaying the expression profile of CD44v6 and ALDH1 showed differential distribution of these markers at the tumor and non-tumor interface in our 3-D models.

Conclusions: 3D tumor reconstructions co-localized with relevant biomarkers have the potential to significantly enhance our understanding of tumor invasion by revealing the additional structural changes or spatial features not appreciated on planar morphologies.

1346 p16 Expression in Follicular Dendritic Cell Sarcoma: A Potential Mimicker of HPV-Related Squamous Cell Carcinoma

Lingxin Zhang, Chen Yang, James Lewis, Samir K El-Mofty, Rebecca Chernock. Washington University School of Medicine, St. Louis, MO; Vanderbilt University Medical Center, Nashville, TN.

Background: Follicular dendritic cells sarcomas (FDCSs) are rare and most commonly occur in cervical lymph nodes but can be found at other head and neck and non-head and neck sites. FDCSs bear some histologic resemblance to HPV-related nonkeratinizing squamous cell carcinomas (NK SCCs). Both have spindled to oval nuclei and indistinct cell borders. Furthermore, NK SCC often presents as an isolated neck mass, just like FDCS, without a clinically obvious primary tumor. FDCSs initially misdiagnosed as SCC have been reported. Immunohistochemistry (IHC) is helpful as FDCS expresses dendritic markers such as CD21 and CD23 and is cytokeratin negative. However, NK SCC is common and in most cases IHC is not performed except for surrogate marker HPV testing by p16 IHC. Recently, genetic alterations in cell cycle proteins, including p16 and its negative regulator retinoblastoma (RB), have been found in FDCS. As a result, we speculated that p16 may be overexpressed in a subset of FDCSs.

Design: p16 and RB IHC were performed on archived FDCSs cases. All were positive for CD21 and CD23 and negative for pan-cytokeratin as part of the initial diagnostic evaluation. p16 IHC was scored for distribution (percent of cells positive) and intensity (weak, moderate, strong). RB was interpreted as retained or lost. A pilot study of CD21 and CD23 in 10 cases of p16-positive NK SCC was performed for comparison.

Results: Of 8 FDCSs, patients' age ranged from 29 to 62 years (mean, 43.5 years), with a M:F ratio of 3:5. Four (50%) had nuclear and cytoplasmic p16 expression, two of which (25%) showed loss of nuclear RB expression (Table 1). All 10 NK SCCs were negative for CD21 and CD23.

Location	p16		RB
	Extent	Intensity	
Neck	-	-	+
Parapharyngeal space	60%	Moderate-Strong	Partial loss
Lung	-	-	+
Rectum	100%	Strong	Loss
Abdomen	80%	Weak-Strong	+
Lung	-	-	+
Nasopharynx	80%	Moderate	+
Retroperitoneum	-	-	+

Conclusions: p16 expression, in some cases likely due to RB inactivation, is common in FDCS and may occasionally be strong and diffuse, as is typical in HPV-related NK SCC. As such, p16 IHC cannot be used as a diagnostic marker for NK SCC when the differential diagnosis includes FDCS. Unusual patterns of p16 staining should also be interpreted cautiously. Dendritic cell and cytokeratin immunostains can easily separate FDCS from NK SCC.

Hematopathology

1347 Low-Level *BCR-ABL1* Transcripts in B-Lymphoblastic Leukemia/Lymphoma (B-LL) at Diagnosis Are Often Transient, but May Rarely Progress

Nidhi Aggarwal, Raven Brower, Urvashi Surti, Sarah E Gibson. University of Pittsburgh School of Medicine, Pittsburgh, PA.

Background: *BCR-ABL1* is the most common recurrent cytogenetic abnormality in adult B-LL, and is associated with a poor prognosis. Quantitative polymerase chain reaction (qPCR) is a sensitive technique commonly used for disease monitoring in B-LL with *BCR-ABL1*. Limited data exists about the significance of low-level *BCR-ABL1* transcripts by qPCR in B-LL at diagnosis that lacks a detectable *BCR-ABL1* fusion with classical cytogenetics (CCG) or fluorescence in situ hybridization (FISH).

Design: 22 cases of B-LL in adult patients (≥18 years of age) that lacked *BCR-ABL1* with CCG and/or FISH and which had at least 1 relapse specimen were identified from 1/2000-6/2016. qPCR for *BCR-ABL1* minor (mcr) and major (Mcr) transcripts was performed on RNA in 2-4 replicates from relapse blood/bone marrow samples, and in 7/22 cases on initial diagnostic specimens. *BCR-ABL1* expression was compared to cell lines (SupB15 for mcr, K562 for Mcr), and was called positive if present in at least 2 of the replicates. Clinical data from these cases was compared to that from 13 adult B-LL with *BCR-ABL1* detected by CCG and/or FISH (high-level *BCR-ABL1*).

Results: 5/22 B-LL (3 male, 2 female; median age 55 years) had low-level *BCR-ABL1* (mcr) transcripts (median 0.0065% SupB15, range 0.0014-6.7%) at diagnosis. Low-level *BCR-ABL1* was transient in 3/5, and persistent in 2/5. In 1/2 cases with persistent *BCR-ABL1*, the transcripts remained at a low-level (≤0.012% SupB15) in relapse specimens. The second case had a low-level transcript at first relapse (5.0% SupB15), but then developed high-level (CCG/FISH+) *BCR-ABL1* at second relapse. There were no statistically significant differences in overall survival or time to relapse between B-LL with low-level *BCR-ABL1* vs B-LL with high-level *BCR-ABL1* or vs B-LL with no *BCR-ABL1* detected ($p>0.05$).